4'-Fluorouridine mitigates lethal infection with pandemic human and highly pathogenic avian influenza viruses

Carolin M Lieber[1], Megha Aggarwal[1], Jeong-Joong Yoon[1], Robert M Cox[1], Julien Sourimant[1], Mart Toots[1], Hae-Ji Kang[1], Scott K Johnson[2], Cheryl A Jones[2], Zachary M Sticher[3], Alexander A Kolykhalov[3], Manohar Saindane[3], Stephen M Tompkins[2], Oliver Planz[4], George R Painter[3], Michael G Natchus[3], Kaori Sakamoto[5], Richard K Plemper[1]*

[1]Center for Translational Antiviral Research, Georgia State University Institute for Biomedical Sciences, Atlanta, GA, 30303, USA.

[2]Center for Vaccines and Immunology, University of Georgia, Athens, GA, 30602, USA

[3]Emory Institute for Drug Development, Emory University, Atlanta, GA, 30329, USA

[4]Department of Immunology, Interfaculty Institute for Cell Biology, Eberhard Karls University Tübingen, Tübingen, Germany

[5]Department of Pathology, College of Veterinary Medicine, University of Georgia, Athens, GA, 30602, USA.

Keywords: influenza virus, pandemic preparedness, antiviral, nucleoside analog, 4'-Fluorouridine

*Corresponding author. Email: rplemper@gsu.edu

Abstract

Influenza outbreaks are associated with substantial morbidity, mortality and economic burden. Next generation antivirals are needed to treat seasonal infections and prepare against zoonotic spillover of avian influenza viruses with pandemic potential. Having previously identified oral efficacy of the nucleoside analog 4'-Fluorouridine (4'-FIU, EIDD-2749) against SARS-CoV-2 and respiratory syncytial virus, we explored activity of the compound against seasonal and highly pathogenic influenza (HPAI) viruses in cell culture, human airway epithelium organoids, and/or two animal models, ferrets and mice, that assess IAV transmission and lethal viral pneumonia, respectively. 4'-FIU inhibited a panel of relevant influenza A and B viruses with nanomolar potency in organoids. *In vitro* polymerase assays revealed immediate chain termination of IAV polymerase after 4'-FIU incorporation, in contrast to delayed chain termination of SARS-CoV-2 and RSV polymerase. Once-daily oral treatment of ferrets with 2 mg/kg 4'-FIU initiated 12 hours after infection rapidly stopped virus shedding and prevented direct-contact transmission to untreated sentinels. Treatment of mice infected with a lethal inoculum of pandemic A/CA/07/2009 (H1N1) (Ca09) with 2 mg/kg 4'-FIU alleviated pneumonia. Three doses mediated complete survival when treatment was initiated up to 60 hours after infection, indicating an unusually broad window for effective intervention. Therapeutic oral 4'-FIU ensured survival of animals infected with HPAI A/VN/12/2003 (H5N1) and of immunocompromised mice infected with pandemic Ca09. Recoverees were fully protected against homologous reinfection. This study defines the mechanistic foundation for high sensitivity of influenza viruses to 4'-FIU and supports 4'-FIU as developmental candidate for the treatment of seasonal and pandemic influenza.

Significance

Next-generation antiviral therapeutics are needed to better mitigate seasonal influenza and prepare against zoonotic virus spillover from animal reservoirs. At greatest risk are the immunocompromised and patients infected with highly pathogenic influenza viruses. This study demonstrates efficacy of a broad-spectrum nucleoside analog, 4'-fluorouridine, against a representative panel of influenza viruses in cell culture, human organoids, and two animal models, ferrets and mice.

Acting as an immediate chain terminator of the influenza virus polymerase, once-daily oral treatment protected against lethal infection with seasonal and highly pathogenic avian influenza viruses, prevented direct-contact transmission to untreated sentinels, and mitigated lethal infection of immunocompromised hosts. These results support the developmental potential of 4'-fluorouridine for treatment of vulnerable patient groups and mitigation of pandemic influenza.

Introduction

Influenza A viruses (IAV) are zoonotic negative sense, segmented RNA viruses with high pandemic potential (1). Wild aquatic birds are a major natural reservoir for avian influenza viruses, creating high opportunity for spread into the poultry industry and spillover of HPAI viruses into the human population with potentially catastrophic consequences (2, 3). The 2021-2022 H5N1 HPAID epidemic specifically is the largest on record, having reached an unprecedented geographical expansion and requiring the culling of 48 million birds so far (4). Approximately 14 IAV pandemics have occurred in the past 500 years (5), six of which were concentrated in the last 120 years alone. Most deadly of these outbreaks was the 1918 "Spanish Flu" pandemic, which was caused by an H1N1 subtype IAV of unusual virulence that accounted for approximately 500 million infected people, equating to nearly a third of the world population at the time, and 50 million death (6). Case fatality rates were particularly high in young children, 20-40 year old adults, and the elderly above 65 years of age (6). Subsequent pandemics in the 20th century included the Asian influenza of 1957 and the Hong Kong influenza of 1968, which were caused by IAV of H2N2 and H3N2 subtypes, respectively (5), and the swine origin H1N1 outbreak of 2009 (7). Although considered less pathogenic than several of the earlier pandemic strains, pdm09 IAV is still estimated to have caused 151,000 to 575,400 deaths worldwide and major economic damage (8).

Influenza viruses cause rapid-onset disease with high fever, cough, body aches, rhinorrhea, and nasal congestion (9). Advance to severe disease is marked by virus invasion of the small airways and viral pneumonia, which can lead to sepsis due to a hyperinflammatory systemic response (10). Other serious complications include myocarditis, encephalitis, myositis, and multi-organ failure (11, 12). At

54 greatest risk of life-threatening influenza are children less than 2 years of age, older adults, pregnant
55 women, and patients with pre-existing conditions such as asthma, diabetes, or chronic heart disease
56 (13). Vaccine prophylaxis is available, but the efficacy of the seasonal tetravalent influenza vaccine is
57 moderate, ranging from 40 to 60% even under optimal conditions in interpandemic years (14).
58 Effectiveness of the vaccine can be substantially lower in older adults, who are at greatest risk of
59 progressing to severe disease, or when vaccine components and circulating strains are poorly matched
60 (14). Multiple avenues are being pursued to develop a broad-spectrum influenza vaccine, but none
61 have yet achieved regulatory approval (15).

62 To improve disease management especially in vulnerable patient groups, rapidly respond to
63 endemic outbreaks of seasonal influenza when the vaccine is not optimally matched, and to prepare for
64 the pandemic threat originating from zoonotic transmission of HPAI viruses, effective therapeutics with
65 a higher barrier against viral resistance are urgently needed. Three classes of antiviral drugs have
66 received approval by the FDA for treatment of influenza thus far. The M2 channel blocking
67 adamantanes (amantadine and rimantadine), the neuraminidase inhibitors (oral oseltamivir, inhaled
68 zanamivir, intravenous peramivir), and, most recently, the PA endonuclease inhibitor baloxavir marboxil
69 (16). Of these, use of the adamantanes has been discontinued due to widespread pre-existing
70 resistance in human influenza viruses and natural IAV reservoirs (17). Pre-existing signature resistance
71 mutations against the neuraminidase inhibitors were furthermore detected in 2009 pandemic viruses
72 (18), giving rise to the concern that future effectiveness of this inhibitor class may be questionable (19).
73 Although baloxavir marboxil is the newest influenza drug, resistance has developed rapidly and was
74 even observed in human patients during the early clinical trials, resulting in rebound of virus replication
75 (20-22). Novel therapeutic options are therefore needed to broaden the available anti-influenza virus
76 drug arsenal.

77 In search of suitable broad-spectrum developmental candidates, we explored in this study antiviral
78 potency, *in vivo* efficacy, and mechanism of action of 4'-FIU against the influenza virus indication.
79 Recently, we reported that 4'-FIU is a highly potent inhibitor of SARS-CoV-2 and pathogens of the
80 mononegavirus order (23, 24), establishing oral efficacy in animal models of SARS-CoV-2 and

81 respiratory syncytial virus (RSV) infection. Having demonstrated that this nucleoside analog functions
82 as an immediate chain terminator of influenza virus polymerase, we assessed oral efficacy in two
83 different animal models, mice and ferrets, against pandemic human and HPAI viruses. Influenza
84 treatment paradigms developed in these models outline an unusually broad time window for successful
85 therapeutic interference with a lethal viral challenge. These results support the development of 4'-FIU
86 as a therapeutic candidate for the treatment of influenza with the potential to improve preparedness
87 against zoonotic spillover of avian IAVs with pandemic potential into the human population.
88

89 **Results**

90 To explore whether the indication spectrum of 4'-FIU (figure 1a) extends to the orthomyxoviruses,
91 we examined activity of the compound against seasonal and pandemic IAVs representing H1N1 and
92 H3N2 subtypes and against a representative influenza B virus (IBV) isolate in cell culture (figure 1b). In
93 parallel, we generated human airway epithelium organoids grown at air-liquid interface from a healthy
94 donor and tested inhibition of pandemic Ca09 through basolateral 4'-FIU (figure 1c), and determined
95 activity against a recombinant A/WSN/33 (H1N1)-based reporter virus (25) on non-differentiated
96 primary HAE cells representing 10 distinct donors (supplementary figure S1). All viral isolates tested
97 were highly sensitive to the compound, returning 50% and 90% inhibitory concentrations (EC_{50} and
98 EC_{90}, respectively) in the low-nanomolar range with steep Hill slopes. Combined with a 50% cytotoxic
99 concentration (CC_{50}) of 4'-FIU of 468 μM (23) in primary HAEs from the same donor as used in the
100 organoid model, we calculated a selectivity index (SI = CC_{50}/EC_{50}) of 4'-FIU against pandemic Ca09 of
101 187,200 in this disease-relevant human tissue model.

102 **4'-FIU is an immediate chain terminator of influenza virus polymerase**

103 Through biochemical RdRP assays using purified recombinant RSV and SARS-CoV-2 polymerase
104 complexes and synthetic template RNA, we have demonstrated that incorporation of 4'-FIU
105 triphosphate (4'-FIU-TP) into nascent chain RNA triggers delayed termination of the RNA-dependent
106 RNA polymerases from a negative sense (RSV) and a positive sense (SARS-CoV-2) RNA virus.
107 Whereas variations in stalling efficiencies were observed between sequences and polymerase, position

108 *i*+3 marked the predominant stalling site (23). Following expression of IAV RdRP PA, PB1, and PB2
109 subunits in insect cells, we subjected affinity chromatography purified, reconstituted IAV polymerase to
110 the equivalent biochemical RdRP assay in the presence of increasing concentrations of 4'-FIU-TP or
111 UTP (figure 1d-e, supplementary figure S2a-e). 4'-FIU-TP was incorporated instead of UTP when the
112 polymerase reached the first adenosine in the template RNA as we had noted before in RSV and
113 SARS-CoV-2 RdRP assays (23), but then triggered immediate chain termination of IAV RdRP.
114 Densitometric quantitation of relative amplicon intensities to compare incorporation rates of the analog
115 relative to UTP revealed an approximately 4-fold higher affinity of IAV polymerase for endogenous UTP
116 than for 4'-FIU-TP (figure 1f).

117 These results demonstrate high sensitivity of influenza virus polymerases to 4'-FIU and identify
118 sequence-independent immediate chain termination at position *i* as a predominant mechanism of
119 influenza virus RdRP inhibition by the compound.

120 **Pharmacokinetic (PK) properties of 4'-FIU in mouse plasma and tissues**

121 We have previously demonstrated oral bioavailability of 4'-FIU in ferrets and efficient intracellular
122 anabolism to 4'-FIU-TP with prolonged tissue exposure levels (23). To assess cross-species
123 conservation of PK profiles between IAV efficacy models used in this study, ferrets and mice, we
124 subjected the compound to a single-dose oral PK study in mice, measuring 4'-FIU plasma
125 concentrations and corresponding 5'-triphosphate levels in selected soft tissues after oral dosing at 1.5
126 mg/kg body weight (figure 2a-b). Free 4'-FIU reached a maximal plasma exposure of approximately 1
127 μM 90 minutes after oral administration, far exceeding the cell culture EC_{90} concentration against the
128 influenza virus test panel. Plasma levels were sustained high over a 12-hour period after dosing.
129 Corresponding 4'-FIU-TP tissue exposure levels 12 hours after dosing were approximately 1 nmol/g
130 tissue in all organs but brain and kidney, underscoring suitability of 4'-FIU for *in vivo* efficacy testing
131 against IAV.

132 **Late-onset treatment with 4'-FIU mediates complete survival of IAV-infected animals**

133 For mouse efficacy studies, animals were infected intranasally with a lethal inoculum amount of
134 pandemic Ca09, which replicates efficiently in mice without a requirement for species adaptation (26).

135 Infection results in severe viral pneumonia with major clinical signs such as weight loss and
136 hypothermia. To establish the lowest efficacious dose, we examined 3 4'-FIU dose levels in a survival
137 study, each administered by oral gavage on three consecutive days in a once daily (q.d.) regimen
138 starting at the time of infection (figure 2c). All animals treated at the 2 mg/kg dose level survived,
139 whereas all mice of the vehicle-treated and lowest dose (0.08 mg/kg) groups succumbed to infection
140 within 5 days of inoculation (figure 2d) and experienced clinical signs (supplementary figure S3a-b).
141 Animals receiving the intermediate 4'-FIU dose (0.4 mg/kg) had prolonged survival, but ultimately all
142 died.

143 Having established 2 mg/kg 4'-FIU administered q.d. as a low efficacious dose, we next
144 determined the latest time for initiation of effective treatment at this dose level (figure 2e). All vehicle-
145 treated animals again succumbed to infection within 5 days of inoculation (figure 2f). In contrast,
146 treatment start at 2.5 days after infection, which corresponds to 0.5 days after the onset of major clinical
147 signs (supplementary figure S3c-d) ensured complete survival, and 80% of animals of a group receiving
148 the first dose 3 days after infection survived, outlining a broad therapeutic time window for treatment of
149 influenza with 4'-FIU. Therapeutic benefit of late-onset treatment was corroborated by a significant
150 reduction in lung virus load compared to vehicle-treated controls at 4.5 days after infection, determined
151 in a parallel set of equally treated animals (figure 2g). Within 7 days, virus became undetectable in
152 lungs of animals that were treated starting 24 hours after infection with oral 4'-FIU (2 mg/kg q.d.; 3
153 doses total), indicating that viral replication had ceased (figure 2h). No rebound of virus replication was
154 observed within a 9-day period after infection (supplementary figure S3e-f). These results define a
155 broad therapeutic time window for effective treatment of IAV infection with 4'-FIU.

156 To determine the minimal number of oral 4'-FIU doses (2 mg/kg q.d.) for complete survival, we
157 again initiated treatment 24 hours after infection, in this study comparing the effect of a single vs double
158 or triple doses (figure 2i). Lung virus load was assessed 4.5 days after infection and survival monitored
159 in a parallel set of equally treated animals. The number of doses administered correlated with antiviral
160 effect size, but even a single dose of 4'-FIU resulted in a statistically significant reduction in lung virus
161 load of approximately one order of magnitude (figure 2j). Reduced viral burden translated to survival of

162 some animals in the single and double dose groups. However, three doses were required for full
163 therapeutic benefit (figure 2k) and only mild clinical signs (supplementary figure S3g-h).

164 **4'-FIU effect on IAV transmission in the ferret model**

165 Since mice, in contrast to ferrets, do not shed IAVs, we next explored anti-IAV efficacy of 4'-FIU in
166 the ferret model. Guided by the dosing regimen established in mice, we treated animals infected
167 intranasally with Ca09 with either 2 mg/kg (standard dose) or 0.5 mg/kg (low dose), administered orally
168 starting 24 hours after infection (figure 3a). Animals received one (2 mg/kg level) or two doses (either 2
169 or 0.5 mg/kg level) total. Fever is the predominant clinical sign associated with Ca09 IAV infection in
170 ferrets. Monitoring body temperature continuously telemetrically, we observed significant reduction in all
171 treated animals within 24 hours of the first dose, whereas vehicle-treated animals showed a prolonged
172 fever plateau (supplementary figure S4a). Viral titers in nasal lavages were statistically significantly
173 reduced compared to those of vehicle animals, but effect size was lower in animals of the low dose
174 than the standard dose group, and virus rebounded 2.5 days after infection in the single standard dose
175 group (figure 3b). In contrast, two standard doses 4'-FIU given q.d. were sterilizing within 2 days of
176 treatment initiation. Virus load in nasal turbinates assessed 4 days after infection corroborated the
177 lavage titers, revealing a dose-dependent significant antiviral effect of two doses, whereas a single
178 dose had no significant effect on virus titer in turbinates at the time of tissue harvest (figure 3c).
179 Examination of lower respiratory tract tissues, trachea, and bronchoalveolar lavage fluid (BALF)
180 revealed, however, that a single standard dose of 4'-FIU administered at the time of onset of clinical
181 signs completely suppressed the development of viral pneumonia (figure 3d).

182 To determine the effect of 4'-FIU on virus spread, we treated in a direct-contact transmission study
183 source ferrets infected with Ca09 with the compound as before, starting 12 or 24 hours after infection
184 (figure 3e). Co-housing of source ferrets with untreated sentinels in a 1:1 ratio was initiated 2.5 days
185 after study start. Ca09 rapidly spread from vehicle-treated source ferrets to their direct contacts, which
186 first became virus-positive in nasal lavages only 12 hours after the beginning of co-housing (figure 3f)
187 and had progressed to viral pneumonia with high turbinate, lung and trachea virus load by study end
188 (figure 3g-h) and clinical signs (supplementary figure S4b-e). Treatment of source animals with 4'-FIU

189 initiated 12 or 24 hours after infection in each case resulted in exponential decline in shed virus load,
190 but virus was undetectable in lavages of the 12-hour treatment group by the time of co-housing
191 whereas approximately 10^4 $TCID_{50}$ units/ml lavage remained detectable in lavages of the 24-hour
192 treatment group at that time. We did not detect any virus transmission to untreated sentinels of the 12-
193 hour group. However, low-grade transmission to direct contacts of the 24-hour treatment group
194 occurred, characterized by delayed onset of virus shedding compared to sentinels of vehicle-treated
195 source animals and a reduced peak shed virus load (figure 3h). Shedding from all sentinels that
196 became virus-positive ceased approximately 12 days after the beginning of co-housing. These results
197 confirm cross-species anti-IAV efficacy of 4'-FIU, reveal that a single oral dose is sufficient to prevent
198 advance to severe influenza, and demonstrate a shortened window in which a treated case remains
199 fully infectious.

200 **Mitigation of IAV pathogenesis and lung histopathology by 4'-FIU**

201 To better understand the impact of 4'-FIU on mitigating immunopathogenesis, the major driver of
202 clinical signs associated with influenza virus infection, we determined inflammatory cytokine profiles for
203 a 10-day period after infection of mice with Ca09 using a 6-plex Th17 cytokine assay (figure 4a).
204 Treated animals received the 3-dose standard 4'-FIU regimen as before, started 24 hours after
205 infection. Lung tissue for histopathology was extracted from parallel sets of equally treated animals 5 or
206 21 days after infection. Lung titers in vehicle-treated animals demonstrated fast-onset viral pneumonia,
207 approaching a burden of 10^6 infectious units/g lung tissue 4 days after infection, when all animals of the
208 vehicle group had succumbed to infection with major clinical signs (figure 4b, supplementary figure
209 S5a-b). Pro-inflammatory cytokines rapidly increased in the BALF of these animals, revealing a very
210 strong antiviral response until death of the vehicle animals as expected after infection with Ca09 (figure
211 4c-d, supplementary figure S6). Treatment with 4'-FIU again efficiently suppressed virus replication
212 within 24 hours of the first dose (figure 4b). Coinciding with the reduction in virus burden of treated
213 animals by approximately two orders of magnitude by day 3 after infection, the proinflammatory
214 response was greatly alleviated (figure 4c-d, supplementary figure S6) and all treated animals survived
215 (supplementary figure S5a).

216 Consistent with a better clinical outcome (supplementary figure S7a-b), lowered viral load, and
217 mitigated innate antiviral response in 4'-FIU treated vehicle animals, analysis of lung histopathology 5
218 days after infection revealed reduced lung lesions and alleviated cellular infiltrates in lung tissue of
219 treated animals (figure 4e, supplementary figure S8). Overall combined histopathology scores of
220 individual animals representing the degree of cellular infiltrates into alveoli and bronchioles, the extent
221 of perivascular cuffing, and the severity of interstitial pneumonia, pleuritis, and vasculitis were
222 statistically significantly lower in the treatment than vehicle group (figure 4f, supplementary figure S9).

223 **4'-FIU control of influenza in immunocompromised hosts and of HPAI infection**

224 In the clinic, the risk of progression to severe disease and poor overall outcome is greatly
225 increased when immunocompetence of the patient is impaired or after zoonotic spillover of HPAIs into
226 the human population (27, 28). To first assess the potential of 4'-FIU to pharmacologically manage
227 influenza in high-risk hosts, we infected interferon α/β receptor knockout (IFNAR1 KO) and V(D)J
228 recombination activation gene RAG-1 KO mice with Ca09. Whereas the former cannot mount an
229 effective type I IFN innate response (29, 30), the latter are compromised in their cell-mediated adaptive
230 immunity due to a lack of mature T and B cells (31). Oral treatment with 4'-FIU was initiated 24 hours
231 after infection at standard and a high-dose (10 mg/kg) level, then continued q.d. for a total of 7 doses of
232 each group (figure 5a). Independent of 4'-FIU dose level, all treated animals of the RAG-1 KO and
233 IFNAR1 KO groups survived, whereas all animals in the vehicle-treated groups developed severe
234 clinical signs (supplementary figure S10a-d) and succumbed to infection within 4 days (figure 5b).
235 Reduction in lung virus load of treated vs vehicle animals after three q.d. 4'-FIU doses (day 4 after
236 infection) was dose level-dependent, but even at the standard dose, this reduction exceeded two orders
237 of magnitude in either knockout mouse strain (figure 5c).

238 Next, we explored 4'-FIU efficacy against HPAIs, initially testing potency against polymerases
239 derived from A/CA/07/2009 (H1N1), A/VN/12/2003 (H5N1), and A/Anhui/1/2013 (H7N9) in minireplicon
240 dose-response assays (figure 5d). The compound dose-dependently inhibited activity of either HPAI-
241 derived polymerase complex, reaching active concentrations resembling that observed against Ca09
242 RdRP. Selecting A/VN/12/2003 (H5N1), which causes lethal encephalitis in mice (32), for a proof-of-

243 concept efficacy study of 4'-FIU against zoonotic HPAIs, we started treatment at the 5 mg/kg dose level
244 12 or 24 hours after infection and continued q.d. thereafter (figure 5e). None of the animals of either 4'-
245 FIU treatment group developed clinical signs even when treatment was initiated 24 hours after infection
246 (figure 5f), and all treated animals survived (figure 5g). In contrast, all vehicle-treated animals
247 succumbed to A/VN/12/2003 (H5N1) with a median survival time of 9 days after infection, developing
248 clinical signs on day 7 after infection followed by rapid further deterioration (figure 5f). Vehicle-treated
249 animals experienced high lung virus loads three days after infection (figure 5h). Treatment reduced
250 HPAI burden by several orders of magnitude to limit of detection. These results confirm
251 uncompromised efficacy of 4'-FIU in high-risk immunocompromised hosts and against highly
252 pathogenic zoonotic viruses with high pandemic concern.

253 **Anti-IAV immune status of 4'-FIU-treated recoveries**

254 Highly efficacious antivirals may suppress host immune activation, especially when treatment is
255 started early in the course of infection, which may leave the host susceptible to subsequent re-infection
256 and may potentially even result in exacerbated disease (33-35). To explore the effect of 4'-FIU on
257 subsequent homotypic IAV rechallenge of recoveries, we infected animals with Ca09 and started
258 standard 3-dose 4'-FIU treatment at three time points, therapeutically at 24 and 48 hours after infection
259 and prophylactically at 12 hours before infection (figure 6a). For this study, mice were inoculated with
260 aerosolized virus in a temperature and airflow-controlled aerosol chamber using an Aeroneb nebulizer
261 (supplementary figure S11a-b) to better mimic natural infection. Prior to study start, we performed pilot
262 experiments to determine suitable exposure time (supplementary figure S12a-c), infectious dose
263 (supplementary figure S13a-b) and proof-of-concept for 4'-FIU efficacy (supplementary figure S14a-d)
264 after infection with aerosolized virus. Mirroring the outcome of our previous efficacy studies, animals of
265 all treatment groups survived the original infection, whereas all animals of the vehicle group reached
266 predefined clinical endpoints 9 days after infection and had to be terminated (figure 6b) with major
267 clinical signs (supplementary figure S15a-b). To assess the status of humoral anti-Ca09 immunity, we
268 collected blood samples from the treated recoverees 4, 8, and 12 weeks after the original infection and
269 determined neutralizing antibody (nAb) titers. Mice in both therapeutic treatment groups mounted a

270 robust humoral anti-IAV response, whereas no nAbs were detectable in the prophylactically treated
271 animals 8 weeks after the original infection (figure 6c). Upon homotypic rechallenge with aerosolized
272 Ca09 10 weeks after the original infection, however, all 4'-FIU-experienced recoverees had a significant
273 benefit over a new set of IAV-naïve mice (figure 6d). All animals of the therapeutic groups survived with
274 significant boost in nAb titers relative to week 8 levels. Remarkably, four of the five animals treated
275 prophylactically with 4'-FIU at the time of the original infection also survived the homotypic rechallenge
276 and mounted a robust humoral anti-Ca09 response by week 12. In contrast, all newly added IAV-
277 inexperienced animals succumbed to infection within 9 days, confirming efficient virus delivery through
278 aerosolization at rechallenge. Animals of the treatment group remained disease-free during
279 rechallenge, and clinical signs were alleviated in mice of the prophylactic group (supplementary figure
280 S15c-d). Independent of the original 4'-FIU regimen applied, we did not detect any signs of exacerbated
281 disease upon rechallenge of treatment-experienced recoverees.
282

283 **Discussion**

284 Treatment of influenza has remained challenging, despite the current availability of two different
285 FDA-approved drug classes, the neuraminidase and endonuclease inhibitors (36). The main challenges
286 to more successful antiviral therapies are narrow therapeutic time windows (37), poor patient
287 compliance (38), and impaired immunocompetence of older adults at greatest risk of advance to severe
288 disease (39), defining key developmental objectives for the next generation of influenza therapeutics.
289 Demonstrating antiviral potency in cell culture, human airway organoids, and/or efficacy in two
290 relevant *in vivo* infection models, ferrets and mice, this study establishes oral efficacy of 4'-FIU, a
291 broad-spectrum antiviral ribonucleoside analog (23, 24), against seasonal, pandemic, and HPAI IAV
292 strains. Designed to expand our first-line pharmacological arsenal against RNA viruses of pandemic
293 concern, we have previously shown activity of 4'-FIU against SARS-CoV-2, pneumoviruses such as
294 RSV and paramyxoviruses (23). Mechanistic characterization consistently demonstrated that
295 incorporation of 4'-FIU-TP into the nascent RNA strand induces polymerase chain termination (23).
296 Unique to 4'-FIU of all chain-terminating ribonucleoside analogs analyzed (24), however, the modus of

297 4'-FIU-induced termination varies dependent on RdRP target. IAV RdRP stalled immediately upon
298 incorporation, RSV polymerase termination was delayed at position *i*+3 after incorporation, and SARS-
299 CoV-2 polymerase termination was delayed and dependent on sequence context, requiring
300 incorporation of at least two 4'-FIU moieties in close repetition (23). Delayed chain termination typically
301 reflects that incorporation of the nucleoside analog alters secondary structure of the nascent strand,
302 which interferes with polymerase processivity (24, 40, 41). Accordingly, we hypothesize that distinct
303 mechanisms of action (MOAs) against betacoronaviruses, pneumoviruses, and orthomyxoviruses are
304 due to different capabilities of the respective polymerase complexes to accommodate 4'-FIU-specific
305 secondary structure changes.

306 In clinical trials of baloxavir marboxil, viral resistance emerged rapidly, resulting in rebound of virus
307 replication in 82.1% of treated patients (22). Whole genome sequencing of 4'-FIU-experienced virus
308 populations isolated from infected and treated animals showed no allele-dominant divergence from the
309 inoculum population, suggesting a high genetic barrier against resistance to 4'-FIU (23). It will
310 nevertheless be exciting to explore whether future resistance profiling of the compound against different
311 viral targets, including IAV, RSV, and SARS-CoV-2, is feasible and may illuminate residues that control
312 structural flexibility of the polymerase complexes rather than substrate specificity.

313 Very likely representing a direct consequence of the distinct MOAs, however, we found influenza
314 viruses to be most sensitive to inhibition by 4'-FIU, followed by RSV and SARS-CoV-2. Dose-finding in
315 the mouse model identified effective levels in the low mg/kg range and three doses administered q.d. to
316 be sufficient for achieving full therapeutic benefit, which resembled efficacy performance of baloxavir
317 marboxil (42) and far outpaced that of the neuraminidase inhibitors (43). Whereas therapeutic
318 oseltamivir lacked efficacy in mice infected with pdm09 IAV isolates (44) and baloxavir marboxil
319 ensured only partial survival when treatment was started later than 24 hours after infection (42),
320 treatment with 4'-FIU mediated unprecedented complete survival of all treated animals when the
321 inhibitor was first administered as late as 60 hours after infection, at the time when lung virus burden
322 approached peak titer (45) and major clinical signs had manifested. If predictive of the treatment of
323 human disease, this substantially widened therapeutic time window may be game-changing for

324 influenza therapy.

325 Since clinical signs of influenza are largely a result of immunopathogenesis (46), we asked
326 whether 4'-FIU may impact the quality of the antiviral immune response and potentially trigger
327 exacerbated disease upon homotypic re-infection. Cytokine profiling showed an alleviated pro-
328 inflammatory response in animals dosed therapeutically with 4'-FIU, but assessment of neutralizing
329 antibody titers revealed that each of the treated animals had mounted a robust humoral response.
330 Consistent with our previous observation of low cytotoxic and cytostatic potential of 4'-FIU (23), these
331 results indicate that mitigated immunopathogenesis in treated animals is a consequence of reduced
332 virus load rather than a direct immunomodulatory effect of the compound. Although essentially
333 sterilizing, even prophylactic treatment resulted in partial protection of animals at re-infection despite
334 the absence of neutralizing antibodies, indicating that treated animals also mounted a viable cell-
335 mediated adaptive response (47, 48).

336 Beyond individual patient benefit through mitigation of lethal infection and alleviation of viral
337 pneumonia and lung immunopathogenesis, 4'-FIU statistically significant reduced upper respiratory
338 tract virus load and viral shedding when treating 12 hours after infection, resulting in fully suppressed
339 spread to untreated direct-contact sentinels in the highly sensitive ferret transmission model (49). Later
340 treatment initiation still reduced transmission efficiency, resulting in delayed onset of virus replication
341 and reduced upper respiratory tract peak virus load, which serves as a biomarker for risk of progression
342 to severe viral pneumonia (50). If equally applicable to the human host, pharmacological block or
343 mitigation of transmission provides a promising path towards outbreak control through efficient
344 interruption of community transmission chains, mitigating the health threat and economic burden (51) of
345 endemic and pandemic influenza.

346 At greatest risk of life-threatening disease are the immunocompromised (52, 53) and patients
347 infected with zoonotic HPAI viruses (54, 55). When assessed in an immunocompromised mouse
348 model, baloxavir marboxil returned a significantly prolonged time to death, but ultimately all animals
349 succumbed to the infection (56). In contrast, treatment with 4'-FIU mediated complete survival of all
350 animals in two distinct immunocompromised mouse models, underscoring powerful antiviral activity that

351 does not strictly depend on a fully immunocompetent host to clear the infection (57). Adding efficient
352 control of highly pathogenic zoonotic IAVs, we propose that 4'-FIU meets key efficacy requirements of a
353 next-generation antiviral clinical candidate that strengthens pandemic preparedness and provides a
354 much-needed alternative option for management of seasonal and pandemic influenza viruses.
355

356 **Material and Methods**

357 **Study design**

358 Cells, ferrets and mice were used as *in vitro*, *ex vivo* and *in vivo* models, respectively, to examine
359 efficacy of 4'-FIU against Influenza infections. Biochemical RdRP assays were added for mechanistic
360 characterization against the influenza virus target. Viruses were administered through intranasal or
361 aerosolized (mice only) inoculation and virus load monitored periodically in nasal lavages (ferrets only),
362 and in respiratory tissues of ferrets and mice extracted 4 days and 3-14 days, respectively, after
363 infection. Virus titers were determined through $TCID_{50}$-titration.

364 **Cells, viruses, and compound synthesis**

365 MDCK (ATCC CCL-34) and 293T (ATCC CRL-3216) cells were cultured in Dulbecco's modified
366 Eagle's medium (DMEM) supplemented with 7.5% heat-inactivated fetal bovine serum (FBS) at 37°C
367 and 5% CO_2. Human primary cells were grown in epithelial differentiation medium (23). A/Alberta/35/76
368 (H1N1), A/Spain/53207/2004 (H1N1), A/Wisconsin/67/2005 (H3N2), A/CA/07/2009 (H1N1),
369 A/Netherlands/602/2009 (H1N1), A/WSN/33 (H1N1), and A/Wyoming/03/2003 (H3N2), as well as
370 B/Brisbane/60/08 were propagated on MDCK cells using serum-free DMEM supplemented with 0.5%
371 Trypsin. A/Viet Nam/1203/2004 (H5N1) was propagated in the allantoic cavity of embryonated hen
372 eggs at 37°C for 24 hours, clarified, aliquoted, and stored at −80°C. The titer of A/Viet Nam/1203/2004
373 (H5N1) was determined by plaque assay on MCDK cells. Virus stock titers were determined through
374 $TCID_{50}$-titration, stocks were stored in aliquots at -80°C. Recombinant influenza viruses were recovered
375 using an 8-plasmid system generated for A/CA/07/2009 (H1N1) that was based on original reports for
376 laboratory-adapted IAV (58). Reporter viruses were generated through insertion of a nanoLuc or
377 maxGFP-encoding ORF in frame at the 5'-end of the viral HA ORF, separated by a 2A cleavage site as

378 described for other recombinant IAVs (59). Genetic stability of the resulting nanoLuc-HA and maxGFP-
379 HA segments was validated through sequence confirmation after 10 consecutive viral passages on
380 MDCK cells. 4'-FIU was synthesized from 5'-(3-chlorobenzoyloxy)-2',3'-di-O-acetyl-4'-fluorouridine and
381 4N ammonia in methanol as previously described (23), authenticated through elemental analysis, and
382 stored as dry powder. Working aliquots were dissolved in DMSO or 10% methylcellulose for *in vitro* and
383 *in vivo* studies, respectively.

384 **Primary human airway epithelium organoid cultures**

385 Primary HAEs (3×10^5/well) at passage <3 were seeded on 6.5 mm 0.4 µm pore size polyester
386 inserts (Corning Costar Transwell) and differentiated for at least 21 days at air-liquid interface using Air-
387 Liquid Interface Differentiation Medium (LifeLine Cell Technology). Transepithelial/transendothelial
388 resistance (TEER) was monitored using an EVOM volt/ohm meter coupled with STX2 electrode (World
389 Precision Instruments). Developing organoids were washed apically at least once per week to remove
390 mucus. For infection virus was added apically, treatment occurred through compound addition to the
391 basolateral chamber.

392 **Virus titration**

393 Virus samples were serially diluted (10-fold starting at 1:10 initial dilution) in serum-free DMEM
394 supplemented with 0.5% Trypsin (Gibco). Serial dilutions were added to MDCK cells seeded in 96-well
395 plate at 1×10^4 cells per well 24 hours before infection. Infected plates were incubated for 72 hours at
396 37°C with 5% CO_2, followed by transfer of culture supernatants to suspension of chicken red blood cells
397 and scoring of wells based on hemagglutination activity. A/Viet Nam/1203/2004 (H5N1) virus and
398 samples were titered by plaque assay; serially diluted 10-fold in DMEM with 2% FBS, added to MDCK
399 cells in 12-well plates and overlaid with DMEM+2% FBS with 1.2% Avicel microcrystalline cellulose.
400 Plates were incubated for 48 hours at 37°C with 5% CO_2, then washed, fixed with methanol:acetone
401 (80:20), and counter-stained with crystal violet to visualize plaques.

402 **Minigenome assay**

403 293T cells were seeded and transfected with 1.0 µg of luciferase-encoding reporter plasmid (25)
404 and 0.5 µg each of PB1, PB2, NP and PA expression plasmids. Three hours post transfection, 4'-FIU or

405 vehicle (DMSO) volume equivalents were added in 3-fold serial dilution series starting at 20 μM 4'-FIU
406 concentration, followed by incubation for 30 hours at 37°C and determination of luciferase activity using
407 a BioTek Synergy H1 multimode plate reader. Relative activities were calculated according to the
408 formula % relative activity = $(RLU_i - RLU_{min})/(RLU_{max} - RLU_{min}) \times 100$, with RLU_i specifying sample
409 luciferase value, RLU_{min} specifying values from equally transfected, vehicle-treated cells that did not
410 receive the PB2 subunit encoding plasmid, and RLU_{max} specifying values from fully transfected, vehicle-
411 treated cells.

412 **Dose-response assays**

413 Active concentrations (EC_{50} and EC_{90}) of 4'-FIU were calculated through 4-parameter variable
414 slope regression modeling of dose-response assay data, derived from minigenome assays, luciferase
415 reporter virus assays, or progeny virus yield ($TCID_{50}$) assays as specified. Test article was in all cases
416 assessed in 3-fold serial dilutions.

417 **Recombinant IAV RdRP expression and purification**

418 A/CA/07/2009 (H1N1)-derived PA, PB1, and PB2 expression plasmids were subcloned into the
419 pFastbac Dual plasmid expression vector (Invitrogen) with polyhedrin promoter control. An TEV
420 protease-cleavable N-terminal hexahistidine-tag was added to the PA subunit to facilitate purification of
421 the complex through affinity chromatography. The individual plasmids were transformed in DH10bac
422 cells and the resulting bacmid transfected into SF9 cells. After virus recovery, SF9 cells were infected
423 with the three individual viruses in the ratio of 1:1:2. Cells were harvested after 72 hours and lysed in
424 lysis buffer (Tris 50 mM pH 7.4, NaCl 300 mM, NP 40 0.5%, protease inhibitor cocktail, glycerol 10%,
425 TCEP 0.5 mM) on ice for two hours, followed by sonication. Clarified supernatant was incubated at 4°C
426 for 1 hour with Ni-NTA beads which were pre-equilibrated with Tris 50 mM pH 7.4, NaCl 300 mM, NP
427 40 0.2%, glycerol 10%, TCEP 0.5 mM containing 20 mM imidazole. After extensive washing with Tris
428 50 mM pH 7.4, NaCl 300 mM, NP 40 0.2%, glycerol 10%, TCEP 0.5 mM containing 20-50 mM
429 imidazole, protein complexes were eluted in buffer Tris 50 mM pH 7.4, NaCl 300 mM, NP 40 0.2%,
430 glycerol 10%, TCEP 0.5 mM containing 250 mM imidazole. Eluted protein fractions were pooled and
431 loaded on heparin HP columns, which were flushed with buffer A (Tris 50 mM pH 7.4, NaCl 250 mM,

432 glycerol 10%), then 0-100% of buffer B (Tris 50 mM pH 7.4, NaCl 1M, glycerol 10%) diluted in buffer A.
433 The polymerase complex peak was observed in ~80% buffer B, which corresponds to approximately
434 900 mM NaCl in the buffer. Peak fractions were collected separately and dialyzed against buffer C
435 (Tris/Cl 50 mM pH 7.4, NaCl 150 mM, glycerol 10%) in dialyzing cassettes at 4°C overnight. Purified
436 protein complexes were harvested, aliquoted and stored at -80°C until use.

437 ***In vitro* RdRP primer extension assay**

438 *In vitro* primer extension assays were carried out essentially as described (23, 60). Briefly, RdRP
439 assay reactions were set up in 20 mM Tris-HCl pH 7.4, 10% glycerol, 1 mM TCEP, 3 mM MnCl2, 2 μM
440 RNA template, 100 μM RNA primer, and nucleotides and 1 μCi of α^{32}P-labelled ATP (Perkin-Elmer) as
441 specified in the figure legends, followed by incubation at 30°C for 10 minutes. Polymerase complexes
442 were added to the reaction and incubation continued for 1 hour at 30°C. Reactions were stopped with 1
443 volume of deionized formamide containing 25 mM ethylenediaminetetraacetic acid (EDTA), followed by
444 a denaturation step at 95°C. Amplicons were fractionated on 20% polyacrylamide gels with 7M urea,
445 using a Tris-Borate-EDTA electrophoresis buffer. Amplicons were visualized by autoradiography, using
446 a storage phosphor screen BAS IP MS 2040 E (GE Healthcare Life Sciences) and Typhoon FLA 7000
447 (GE Healthcare Life Sciences) imager. Densitometry analysis was performed using FIJI 2.1.0. To
448 determine enzyme kinetics (V_{max} and K_m), Michaelis-Menten equation was applied in Prism 9.0.0
449 (GraphPad).

450 **Pharmacokinetic property and tissue distribution profiling in mice**

451 Male and female C57BL/6J mice were rested for 3 days prior to study start. Then, animals were
452 gavaged with 1.5 mg/kg bodyweight 4'-FIU in 10 mM sodium citrate with 0.5% Tween 80, final gavage
453 volume 200 μl. Blood samples (150 μl) were taken at 90 minutes, 3 hours and 12 hours after dosing,
454 cleared (2,000 rpm, 5 minutes, 4°C), and extracted plasma stored at -80°C. Organ samples (lung,
455 brain, spleen, heart, kidney and liver) were harvested 12 hours after dosing and snap-frozen in liquid
456 nitrogen. Animal tissues were homogenized with 70% acetonitrile in water that included internal
457 standards. Animal plasma and tissue concentrations of 4'FIU and 4'-FIU-TP were measured by a

458 qualified LC/MS/MS method in MRM mode on a QTRAP 5500 (Sciex, Santa Clara, CA, USA)
459 instrument.

460 **Intranasal infection of mice**

461 Female or male mice (5-8 weeks of age, Balb/c, RAG1 KO or IFNar KO) were purchased from
462 Jackson Laboratories. Upon arrival, mice were rested for at least 3 days, then randomly assigned to
463 study groups and housed under ABSL-2 or ABSL-3 conditions for infections with A/CA/07/2009 (H1N1)
464 recombinants or A/VN12/2003 (H5N1), respectively. Bodyweight was determined twice daily, body
465 temperature determined once daily rectally. For infections, animals were anesthetized with isoflurane or
466 isoflurane/ketamine (H5N1 challenge only), followed by intranasal inoculation with 2.5×10^{1} $TCID_{50}$
467 units/animal of A/CA/07/2009 (H1N1), 1×10^{3}- 1×10^{5} $TCID_{50}$ units/animal of GFP or nanoLuc expressing
468 reporter virus versions of A/CA/07/2009 (H1N1), or 6×10^{1} of A/VN12/2003 (H5N1). In all cases, virus
469 inoculum was diluted in 50 µl and administered in amounts of 25 µl per nare. Animals were euthanized
470 and organs harvested at predefined time points or when animals reached humane study endpoints.

471 **4'-FIU anti-IAV efficacy studies in mice**

472 Mice were inoculated intranasally with IAV stocks as described, followed by treatment with 4'-FIU
473 at specified dose levels and starting time points through oral gavage. Unless specified otherwise,
474 treatment was continued q.d. Each individual study contained animals receiving equal volumes of
475 vehicle through oral gavage. At study end point, lung tissue was harvested for virus titration or
476 histopathology assessment. For tissue fixation, lungs were perfused using 10% neutral-buffered
477 formalin [10% formalin, NaH_2PO_4 (4 g/liter), and Na_2HPO_4 (6.5 g/liter)], dissected, and fixed for 24
478 hours. Formalin-fixed lungs were transferred to 70% EtOH after 72 hours, embedded in paraffin,
479 sectioned (5-µm thickness), and stained with hematoxylin and eosin. Slides were evaluated by a
480 licensed pathologist. A pathology score range of 0 to 3 was used to evaluate tissue damage. For
481 analysis of proinflammatory cytokine levels through Bioplex, lungs of euthanized mice were lavaged
482 with 1 ml sterile PBS to extract BALFs, and cleared BALF analyzed against the Standard Th17-panel
483 (Bio-Rad) according to the manufacturer's instructions.

484 **Efficacy studies in ferrets**

485 Female ferrets (6-10 months of age) were purchased from Triple F Farms. Upon arrival, ferrets
486 were rested for 1 week, then randomly assigned to study groups and housed in groups of three animals
487 under ABSL-2 conditions. In some studies, animals received a temperature sensor for continued
488 telemetric measurement of body temperature. Otherwise, body temperature was determined rectally
489 once daily. Dexmedetomidine/ketamine anesthetized animals were inoculated intranasally with 1×10^5
490 $TCID_{50}$ units of A/CA/07/2009 (H1N1) in a volume of 300 µl per nare. Nasal lavages were performed
491 twice daily using 1 ml of PBS containing 2× antibiotics-antimycotics (Gibco). Treatment with 4'-FIU
492 through oral gavage followed a q.d. regimen. Ferrets were terminated four days post infection and
493 BALF and organ (lungs, turbinates and tracheas) samples extracted for virus titrations.

494 **Ferret transmission studies**

495 Female ferrets (3-8 months of age) were anesthetized with dexmedetomidine/ketamine and
496 infected intranasally with 1×10^5 $TCID_{50}$ units of A/CA/07/2009 (H1N1) as before. Nasal lavages were
497 performed every 12 hours, bodyweight and temperature determined once daily. Treatment of source
498 animals was initiated 12 or 24 hours after infection at a dose of 2mg/kg bodyweight, and continued q.d.
499 for three doses total. Starting day 2.5 after infection, uninfected and untreated contact animals were
500 added to the infected and treated source ferrets to allow direct-contact transmission, and co-housing
501 continued until termination of the source ferrets on study day 4. Sentinels were subjected to once daily
502 nasal lavages and monitored until study day 10 or, when infectious particles were detected in lavages
503 of contacts of 4'-FIU-treated source animals, study day 14.

504 **Virus titration from tissue samples**

505 Organs were weighed and homogenized in 500 µl PBS using a beat blaster, set to 3 cycles of 30
506 seconds each at 4°C, separated by 1-minute rest periods. Homogenates were cleared (10 minutes at
507 20,000 × g and 4°C), and cleared supernatants stored at -80°C until virus titration. Viral titers were
508 expressed as $TCID_{50}$ units per gram input tissue. For A/VN12/2003 (H5N1), lungs were homogenized
509 using a TissueLyzer (Qiagen), clarified by centrifugation, supernatants aliquoted, and then stored at -
510 80°C. A/VN12/2003 (H5N1) virus titer was determined by plaque assay and expressed as PFU per ml
511 of lung homogenate.

512 **Infection of mice with aerosolized A/CA/07/2009 (H1N1)**

513 An Aeroneb (Kent Scientific) system was used to infect mice (female Balb/c, 6-8 weeks of age)
514 with aerosolized IAV. Conscious animals were transferred to an aerosol chamber placed on a heat pad
515 adjusted to 37°C to prevent condensation, connected to the nebulizer unit (Aeroneb with palladium
516 mesh) and air pump with airflow restrictor. For condition-finding experiments, the nebulizer chamber
517 was loaded with virus inoculum diluted to 1×10^3-1×10^5 $TCID_{50}$ A/CA/07/2009 (H1N1) per ml in sterile
518 PBS, airflow adjusted to 1 l/minute, and animals continuously exposed for 3, 10, or 30 minutes. For
519 treatment studies, conditions were adjusted to 1×10^5 $TCID_{50}$/ml in sterile PBS, 10 minutes exposure
520 time, and 1 l/minute airflow.

521 **Re-infection of 4'-FIU-experienced mice with A/CA/07/2009 (H1N1)**

522 Mice infected with aerosolized A/CA/07/2009 (H1N1) as above were treated q.d. with 4'-FIU or
523 vehicle as specified, and monitored for 10 weeks or until humane endpoints were reached. Blood was
524 collected 4 and 8 weeks after infection and A/CA/07/2009 (H1N1)-neutralizing antibody titers
525 determined. Treated recoverees were reinfected with homotypic, aerosolized A/CA/07/2009 (H1N1) 10
526 weeks after the original infection along with a fresh set of naïve animals, followed by monitoring for an
527 additional 14 days and final blood collection at study end. No treatment was administered after
528 reinfection.

529 **Neutralizing antibody titers in mice**

530 Plasma was prepared from blood samples (2,000 rpm, 10 minutes, 4°C and stored at -80°C until
531 analysis. Heat-inactivated plasma was incubated with 100 $TCID_{50}$ units of A/CA/07/2009 (H1N1)
532 (H1N1) for 90 minutes, followed by serial dilution and transfer to MDCK cells, and plates incubated for 3
533 days at 37°C. Remaining infectivity was visualized through hemagglutination activity on chicken red
534 blood cells.

535 **Statistical analysis**

536 For statistical analysis of studies consisting of only two groups, unpaired two-tailed t-tests were
537 applied. When comparing more than two study groups, 1-way analysis of variance (ANOVA) or 2-way
538 ANOVA with multiple comparison *post hoc* tests as specified were used to assess statistical difference

539 between samples. Statistical analyses were carried out in Prism version 9.4.1 (GraphPad). The number
540 of individual biological replicates (n values) and exact P values are shown in the figures when possible.
541 The threshold of statistical significance (α) was set to 0.05. Source data and statistical analysis are
542 shown in the supplementary dataset files "source data" and "statistical analysis" respectively.

543 **Ethical compliance**

544 All animal work was performed in compliance with the *Guide for the Care and Use of Laboratory*
545 *Animals* of the National Institutes of Health and the Animal Welfare Act Code of Federal Regulations.
546 Experiments involving mice and ferrets were approved by the Georgia State University Institutional
547 Animal Care and Use Committee (IACUC) under protocols A20012 and A21020, respectively. *In vivo*
548 experimentation with HPAI viruses was approved by the University of Georgia at Athens IACUC under
549 protocol A2020 03-033. All experiments using infectious material were approved by the Georgia State
550 University and the University of Georgia at Athens Institutional Biosafety Committees (IBCs) and
551 performed in BSL-2/ABSL-2 or BSL-3/ABSL-3 containment facilities, respectively. Experiments
552 involving HPAI were reviewed and approved by the IBC of the University of Georgia at Athens and
553 were conducted in enhanced biosafety level 3 (BSL3+) containment according to guidelines for the use
554 of select agents approved by the CDC.

555

556 **Acknowledgements and funding sources**

557 We thank AC Lowen for IAV and IBV virus isolates and the Georgia State University Department of
558 Animal Resources for Assistance. This study was supported, in part, by public health service grant
559 AI141222 (to R.K.P.) from the NIH/NIAID.

560

561 **Conflicts of interest**

562 MGN and GRP are coinventors on patent WO 2019/1736002 covering composition of matter and
563 use of 4'-FIU (EIDD-2749) and its analogs as an antiviral treatment. This study could affect their
564 personal financial status. RKP reports contract testing from Enanta Pharmaceuticals and Atea

565 Pharmaceuticals, and research support from Gilead Sciences, outside of the described work. All other
566 authors declare that they have no competing interests.
567

568 **References**

569 1. Greenwood M (1918) THE EPIDEMIOLOGY OF INFLUENZA. *Br Med J* 2(3021):563-566.
570 2. Sendor AB, Weerasuriya D, & Sapra A (2022) Avian Influenza. *StatPearls*, (StatPearls Publishing
571 Copyright © 2022, StatPearls Publishing LLC., Treasure Island (FL)).
572 3. Christie Wilcox TS (2022) Unprecedented Avian Flu Epidemic Could Presage Year-Round
573 Outbreaks.
574 4. ECDC (2022) 2021-2022 data show largest avian flu epidemic in Europe ever, last excessed
575 10/21/2022. (European Centre for Disease Prevention and Control).
576 5. Taubenberger JK, Kash JC, & Morens DM (2019) The 1918 influenza pandemic: 100 years of
577 questions answered and unanswered. *Sci Transl Med* 11(502).
578 6. CDC (2018) History of 1918 Flu Pandemic, last excessed 10/07/2022. (Centers for Disease
579 Control and Prevention).
580 7. Cheung JTL*, et al.* (2022) Influenza A virus transmission in swine farms and during transport in
581 the swine supply chain. *Transbound Emerg Dis* 69(5):e3101-e3110.
582 8. CDC (2019) 2009 H1N1 Pandemic (H1N1pdm09 virus), last excessed 10/07/2022. (Centers for
583 Disease Control and Prevention).
584 9. Yang JH*, et al.* (2015) Predictive Symptoms and Signs of Laboratory-confirmed Influenza: A
585 Prospective Surveillance Study of Two Metropolitan Areas in Taiwan. *Medicine (Baltimore)*
586 94(44):e1952.
587 10. Florescu DF & Kalil AC (2014) The complex link between influenza and severe sepsis. *Virulence*
588 5(1):137-142.
589 11. Kido H, Chida J, Yao M, & Wang S (2010) [Mechanisms of multi-organ failure in severe
590 influenza]. *Nihon Rinsho* 68(8):1565-1573.
591 12. Radovanovic M*, et al.* (2022) Influenza Myopericarditis and Pericarditis: A Literature Review. *J*
592 *Clin Med* 11(14).
593 13. Vousden N & Knight M (2021) Lessons learned from the A (H1N1) influenza pandemic. *Best*
594 *Pract Res Clin Obstet Gynaecol* 76:41-52.
595 14. CDC (2022) Vaccine Effectiveness: How Well Do Flu Vaccines Work?, last excessed 10/05/2022.
596 (Centers for Disease Control and Prevention).
597 15. Pleguezuelos O*, et al.* (2020) Efficacy of FLU-v, a broad-spectrum influenza vaccine, in a
598 randomized phase IIb human influenza challenge study. *NPJ Vaccines* 5(1):22.
599 16. CDC (2022) Influenza Antiviral Medications: Summary for Clinicians, last excessed 10/05/2022.
600 (Centers for Disease Control and Prevention).
601 17. Nelson MI, Simonsen L, Viboud C, Miller MA, & Holmes EC (2009) The origin and global
602 emergence of adamantane resistant A/H3N2 influenza viruses. *Virology* 388(2):270-278.
603 18. Hussain M, Galvin HD, Haw TY, Nutsford AN, & Husain M (2017) Drug resistance in influenza
604 A virus: the epidemiology and management. *Infect Drug Resist* 10:121-134.
605 19. CDC (2016) Antiviral Drug Resistance among Influenza Viruses, last excessed 10/07/2022.
606 (Centers for Disease Control and Prevention).
607 20. Patel MC*, et al.* (2020) Detection of baloxavir resistant influenza A viruses using next generation
608 sequencing and pyrosequencing methods. *Antiviral Res* 182:104906.
609 21. CDC (2022) Influenza Antiviral Drug Baloxavir Marboxil, last excessed 10/03/2022. (Centers for
610 Disease Control and Prevention).

611 22. Ince WL, Smith FB, O'Rear JJ, & Thomson M (2020) Treatment-Emergent Influenza Virus
612 Polymerase Acidic Substitutions Independent of Those at I38 Associated With Reduced Baloxavir
613 Susceptibility and Virus Rebound in Trials of Baloxavir Marboxil. *J Infect Dis* 222(6):957-961.
614 23. Sourimant J*, et al.* (2022) 4'-Fluorouridine is an oral antiviral that blocks respiratory syncytial virus
615 and SARS-CoV-2 replication. *Science* 375(6577):161-167.
616 24. Lieber CM & Plemper RK (2022) 4'-Fluorouridine Is a Broad-Spectrum Orally Available First-
617 Line Antiviral That May Improve Pandemic Preparedness. *DNA Cell Biol* 41(8):699-704.
618 25. Yan D*, et al.* (2015) Replication-Competent Influenza Virus and Respiratory Syncytial Virus
619 Luciferase Reporter Strains Engineered for Co-Infections Identify Antiviral Compounds in
620 Combination Screens. *Biochemistry* 54(36):5589-5604.
621 26. Kiseleva I*, et al.* (2020) Non-Mouse-Adapted H1N1pdm09 Virus as a Model for Influenza
622 Research. *Viruses* 12(6).
623 27. Hayden FG (1997) Prevention and treatment of influenza in immunocompromised patients. *Am J*
624 *Med* 102(3A):55-60; discussion 75-56.
625 28. Kunisaki KM & Janoff EN (2009) Influenza in immunosuppressed populations: a review of
626 infection frequency, morbidity, mortality, and vaccine responses. *Lancet Infect Dis* 9(8):493-504.
627 29. Arimori Y*, et al.* (2013) Type I interferon limits influenza virus-induced acute lung injury by
628 regulation of excessive inflammation in mice. *Antiviral Res* 99(3):230-237.
629 30. Jackson (2022) B6(Cg)-Ifnar1tm1.2Ees/J, last excessed 10/08/2022. (The Jackson Laboratory).
630 31. Jackson (2022) B6.129S7-Rag1tm1Mom/J, last excessed 10/08/2022. (The Jackson Laboratory).
631 32. Bissel SJ*, et al.* (2012) Acute murine H5N1 influenza A encephalitis. *Brain Pathol* 22(2):150-158.
632 33. Sonoguchi T*, et al.* (1986) Reinfection with influenza A (H2N2, H3N2, and H1N1) viruses in
633 soldiers and students in Japan. *J Infect Dis* 153(1):33-40.
634 34. Memoli MJ*, et al.* (2020) Influenza A Reinfection in Sequential Human Challenge: Implications
635 for Protective Immunity and "Universal" Vaccine Development. *Clin Infect Dis* 70(5):748-753.
636 35. CDC (2016) Background and Guidance on the Use of Influenza Antiviral Agents, last excessed
637 10/07/2022. (Centers for Disease Control and Prevention).
638 36. FDA (2020) Influenza (Flu) Antiviral Drugs and Related Information, last excessed 10/03/2022.
639 (U.S. Food and Drug Administration).
640 37. Xiao X*, et al.* (2020) Identification of Potent and Safe Antiviral Therapeutic Candidates Against
641 SARS-CoV-2. *Front Immunol* 11:586572.
642 38. Smith LE*, et al.* (2016) A systematic review of factors affecting intended and actual adherence
643 with antiviral medication as treatment or prophylaxis in seasonal and pandemic flu. *Influenza*
644 *Other Respir Viruses* 10(6):462-478.
645 39. CDC (2022) Influenza Antiviral Medications: Summary for Clinicians, last excessed 10/07/2022.
646 (Centers for Disease Control and Prevention).
647 40. Tchesnokov EP, Obikhod A, Schinazi RF, & Götte M (2008) Delayed chain termination protects
648 the anti-hepatitis B virus drug entecavir from excision by HIV-1 reverse transcriptase. *J Biol Chem*
649 283(49):34218-34228.
650 41. Kokic G*, et al.* (2021) Mechanism of SARS-CoV-2 polymerase stalling by remdesivir. *Nat*
651 *Commun* 12(1):279.
652 42. Fukao K*, et al.* (2019) Baloxavir marboxil, a novel cap-dependent endonuclease inhibitor potently
653 suppresses influenza virus replication and represents therapeutic effects in both immunocompetent
654 and immunocompromised mouse models. *PLoS One* 14(5):e0217307.
655 43. Wong ZX, Jones JE, Anderson GP, & Gualano RC (2011) Oseltamivir treatment of mice before
656 or after mild influenza infection reduced cellular and cytokine inflammation in the lung. *Influenza*
657 *Other Respir Viruses* 5(5):343-350.

658 44. Pizzorno A, Abed Y, Rhéaume C, & Boivin G (2014) Oseltamivir-zanamivir combination therapy
659 is not superior to zanamivir monotherapy in mice infected with influenza A(H3N2) and
660 A(H1N1)pdm09 viruses. *Antiviral Res* 105:54-58.
661 45. Garigliany MM*, et al.* (2010) Influenza A strain-dependent pathogenesis in fatal H1N1 and H5N1
662 subtype infections of mice. *Emerg Infect Dis* 16(4):595-603.
663 46. Gounder AP & Boon ACM (2019) Influenza Pathogenesis: The Effect of Host Factors on Severity
664 of Disease. *J Immunol* 202(2):341-350.
665 47. Iwasaki A & Medzhitov R (2015) Control of adaptive immunity by the innate immune system.
666 *Nat Immunol* 16(4):343-353.
667 48. Chern YJ & Tai IT (2020) Adaptive response of resistant cancer cells to chemotherapy. *Cancer*
668 *Biol Med* 17(4):842-863.
669 49. Stannard HL*, et al.* (2022) Assessing the fitness of a dual-antiviral drug resistant human influenza
670 virus in the ferret model. *Commun Biol* 5(1):1026.
671 50. Lee N*, et al.* (2009) Viral loads and duration of viral shedding in adult patients hospitalized with
672 influenza. *J Infect Dis* 200(4):492-500.
673 51. de Courville C, Cadarette SM, Wissinger E, & Alvarez FP (2022) The economic burden of
674 influenza among adults aged 18 to 64: A systematic literature review. *Influenza Other Respir*
675 *Viruses* 16(3):376-385.
676 52. Health WSDo (2022) Are you at high risk for flu?, last excessed 10/08/2022.
677 53. CDC (2022) Flu Symptoms & Complications, last excessed 10/06/2022.
678 54. CDC (2015) HPAI A H5 Virus Background and Clinical Illness, last excessed 10/07/2022.
679 55. ECDC (2022) Facts about avian influenza in humans, last excessed 10/10/2022. (European Centre
680 for Disease Prevention and Control).
681 56. Kiso M, Yamayoshi S, Murakami J, & Kawaoka Y (2020) Baloxavir Marboxil Treatment of Nude
682 Mice Infected With Influenza A Virus. *J Infect Dis* 221(10):1699-1702.
683 57. Kimura K, Adlakha A, & Simon PM (1998) Fatal case of swine influenza virus in an
684 immunocompetent host. *Mayo Clin Proc* 73(3):243-245.
685 58. Neumann G*, et al.* (1999) Generation of influenza A viruses entirely from cloned cDNAs. *Proc*
686 *Natl Acad Sci U S A* 96(16):9345-9350.
687 59. Nogales A*, et al.* (2019) A Novel Fluorescent and Bioluminescent Bireporter Influenza A Virus
688 To Evaluate Viral Infections. *J Virol* 93(10).
689 60. Carey MF, Peterson CL, & Smale ST (2013) The primer extension assay. *Cold Spring Harb Protoc*
690 2013(2):164-173.
691
692

693 **Figure legends**

694 **Figure 1. *In vitro* potency and MOA of 4'-FIU against influenza viruses**. **a)** Structure of 4'-FIU. **b)**
695 Dose-response assay of 4'-FIU on MDCK cells. Cells were infected with different subtype IAV or with
696 an IBV isolate. Lines represent 4-parameter variable slope regression model, symbols show data
697 median with 95% CI (n=3); EC_{50} and EC_{90} values are given. **c)** Dose-response assay of 4'-FIU on a
698 well-differentiated HAE organoid against Ca09. Compound was added to the basolateral chamber; line
699 connects data median of apically shed virus, error bars represent 95% CI; EC_{50} and EC_{90} values are
700 shown; n=3. **d)** Coomassie blue staining of purified recombinant IAV RdRP proteins after gel

701 electrophoresis and RNA template sequences used in primer extension assays. **e)** *In vitro* RdRP assay
702 in the presence of ^{32}P-ATP, CTP, and UTP or 4'-FIU-TP as indicated. Representative autoradiogram
703 showing the sequence section highlighted by dashed box in (d); the first incorporation of UTP or 4'-FIU-
704 TP is after position *i*=8 of the amplicon (arrow). The sequence of the amplicon and results of
705 phosphoimager-quantitation of relative signal intensities observed in the presence of 11 μM UTP or 4'-
706 FIU-TP are specified to the left and right of the autoradiogram, respectively. Quantitation graph shows
707 mean values of independent experiments (n=3) ± SD; analysis with 1-way ANOVA with Dunnett's *post*
708 *hoc* test; P values are shown in the graph. Uncropped autoradiogram and replicates are provided in
709 supplementary figure S2. **f)** Kinetic analysis of 4'-FIU-TP and UTP incorporation into the amplicon
710 shown in (e) and supplementary figure S2. Lines represent non-linear regression kinetics with
711 Michaelis-Menten model, K_m and V_{max} are shown, error bars represent 95% CI.
712
713 **Figure 2. Treatment paradigms of 4'-FIU in mice**. **a)** Mouse plasma exposure after a single oral dose
714 of 1.5 mg/kg bodyweight. The red area denotes cell culture $EC_{90} \pm 1 \times$ SD against WSN, all donors as
715 shown in (supplementary figure S1a). **b)** Tissue distribution of bioactive anabolite 4'-FIU-TP in animals
716 shown in (a) 12 hours after dosing. **c)** Schematic of dose-to-failure study against standard
717 recA/CA/2009 (H1N1). **d)** Survival of animals treated as specified in (c). Median survival (ms) time in
718 days is specified; Kaplan-Meier simple survival analysis. **e)** Study schematic to determine the
719 therapeutic time window of oral 4'-FIU in mice, using recA/CA/2009-maxGFP-HA (H1N1) as viral target.
720 **f)** Survival of animals treated as specified in (e). Median survival (ms) time in days is specified; Kaplan-
721 Meier simple survival analysis. **g)** Lung viral load of a set of animals treated as in (e) was determined
722 4.5 days after infection. **h)** Time-to-viral-clearance study. Mice were infected and treated with 4'-FIU at
723 2 mg/kg starting 24 hours after infection and continued q.d. Lung virus load was determined in vehicle-
724 treated animals 4.5 days after infection, and in 4'-FIU-treated animals 4.5, 7, and 9 days after infection.
725 **i)** Schematic of minimal-number-of-doses finding study. **j)** Lung viral load of animals treated as in (i),
726 determined 4.5 days after infection. **k)** Survival of a set of animals treated as in (i). Median survival (ms)
727 time in days is specified; Kaplan-Meier simple survival analysis. Columns in (b, g, h, j) represent data

728 medians with 95% CI, symbols specify individual animals; statistical analysis in (g, h, j) with 1-way
729 ANOVA with Dunnett's *post hoc* test.
730
731 **Figure 3. *In vivo* efficacy of 4'-FIU in the ferret transmission model**. **a)** Ferret efficacy study
732 schematic. **b)** Ferret shed viral titers in nasal lavages. Symbols represent data medians with 95% CI; 2-
733 way ANOVA with Tukey's *post hoc* test, P values are specified; n=3. **c-d)** Tissue and BALF viral titers
734 determined 4 days after infection. Columns represent data medians with 95% CI, symbols specify
735 individual animals; 1-way ANOVA with Dunnett's *post hoc* test, P values are specified. **e)** Transmission
736 study schematic. Treatment of source ferrets was started 12 or 24 hours after infection, animals were
737 co-housed with untreated contact ferrets 2.5 days after infection. **f)** Ferret shed viral titers in nasal
738 lavages of source animals and their sentinels. Light blue dashed line marks time of treatment onset;
739 orange box highlights co-housing period. Symbols represent data medians with 95% CI; 2-way ANOVA
740 with Tukey's *post hoc* test, P values are specified (P values in black compare source animals, P values
741 in blue and brown compare contact ferrets). **g-h)** Virus load in nasal turbinates (g) and lung and trachea
742 tissues (h) in source animals, collected 4 days after infection, respectively. Columns represent data
743 medians with 95% CI; symbols show individual animals; unpaired t-test, P values are specified.
744
745 **Figure 4. Effect of 4'-FIU on the antiviral immune response and lung histopathology. a)** *In vivo*
746 Bioplex and histopathology study schematic. **b)** Lung viral titers in animals treated as in (a). **c-d)**
747 Changes in IL-6 (c) and TNF-α (d) levels present in BALF of animals treated as in (a), relative to levels
748 at time of infection. Symbols in (b-d) represent data medians with 95% CI; 2-way ANOVA with Tukey's
749 *post hoc* test; P values are shown. **e)** Representative photomicrographs of lung tissue extracted 5 days
750 after infection of animals treated as in (a). Tissues of two individual animals per study arm are shown at
751 10× magnification; scale bar denotes 100 μm; Br, Bronchiole; Bl, Blood vessel. **f)** Histopathology scores
752 of animals treated as in (a). Lungs were extracted 5 days after infection. Scores for each animal
753 represents a mean of individual alveolitis, bronchiolitis, vasculitis, pleuritis, perivascular cuffing (PVC),
754 and interstitial pneumonia (IP) scores. Columns represent data medians with 95% CI; symbols show

755 mean scores for each individual animal; 1-way ANOVA with Dunnett's *post hoc* test, P values and n
756 values for each study arm are specified.
757
758 **Figure 5. Efficacy of 4'-FIU in an immunocompromised host and against HPAI. a)** Efficacy study
759 schematic in immunocompromised mice, lacking B and T cells (RAG1 KO) or IFN1 receptor function
760 (IFNar1 KO). **b)** Survival study of animals treated as shown in (a). Median survival (ms) time in days is
761 specified; Kaplan-Meier simple survival analysis. **c)** Lung viral load in animals from (a), determined 4.5
762 days after infection. Columns represent data medians with 95% CI; symbols show individual animals; 1-
763 way ANOVA with Dunnett's *post hoc* test, P values are specified. **d)** Dose-response minigenome assay
764 with RdRP complexes derived from IAV subtypes H1N1, H5N1, and H7N9. Lines represent 4-
765 parameter variable slope regression models; symbols show data medians with 95% CI; n=3. EC_{50}
766 concentrations and 95% CI are specified. **e)** Efficacy study schematic of 4'-FIU against HPAI H5N1. **f)**
767 Body weight measurements of animals shown in (e). Symbols represent data means ± SD, normalized
768 to animal body weight at study start. **g)** Survival study of animals infected with HPAI and treated as
769 shown in (e). Median survival (ms) time in days is specified; Kaplan-Meier simple survival analysis. **h)**
770 Lung virus load on day 3 after infection. Columns represent data medians with 95% CI; symbols show
771 individual animals; 1-way ANOVA with Dunnett's *post hoc* test; P values and n values are specified.
772
773 **Figure 6. Reinfection of 4'-FIU-experienced animals with homotypic H1N1**. **a)** Schematic of the
774 treatment and reinfection study. For infection and reinfection, mice received aerosolized Ca09. **b)**
775 Survival study of animals infected, treated, and reinfected as shown in (a). Median survival (ms) time in
776 days is specified; Kaplan-Meier simple survival analysis. **c)** Anti-H1N1 neutralizing antibody (nAb) titers
777 developing in animals from (a). Symbols represent data medians with 95% CI; 2-way ANOVA with
778 Tukey's *post hoc* test; P values are specified. **d)** Survival of animals after re-infection. Median survival
779 (ms) time in days is specified; Kaplan-Meier simple survival analysis. N numbers for animals in (a-d)
780 are specified in (a).

Figure 1

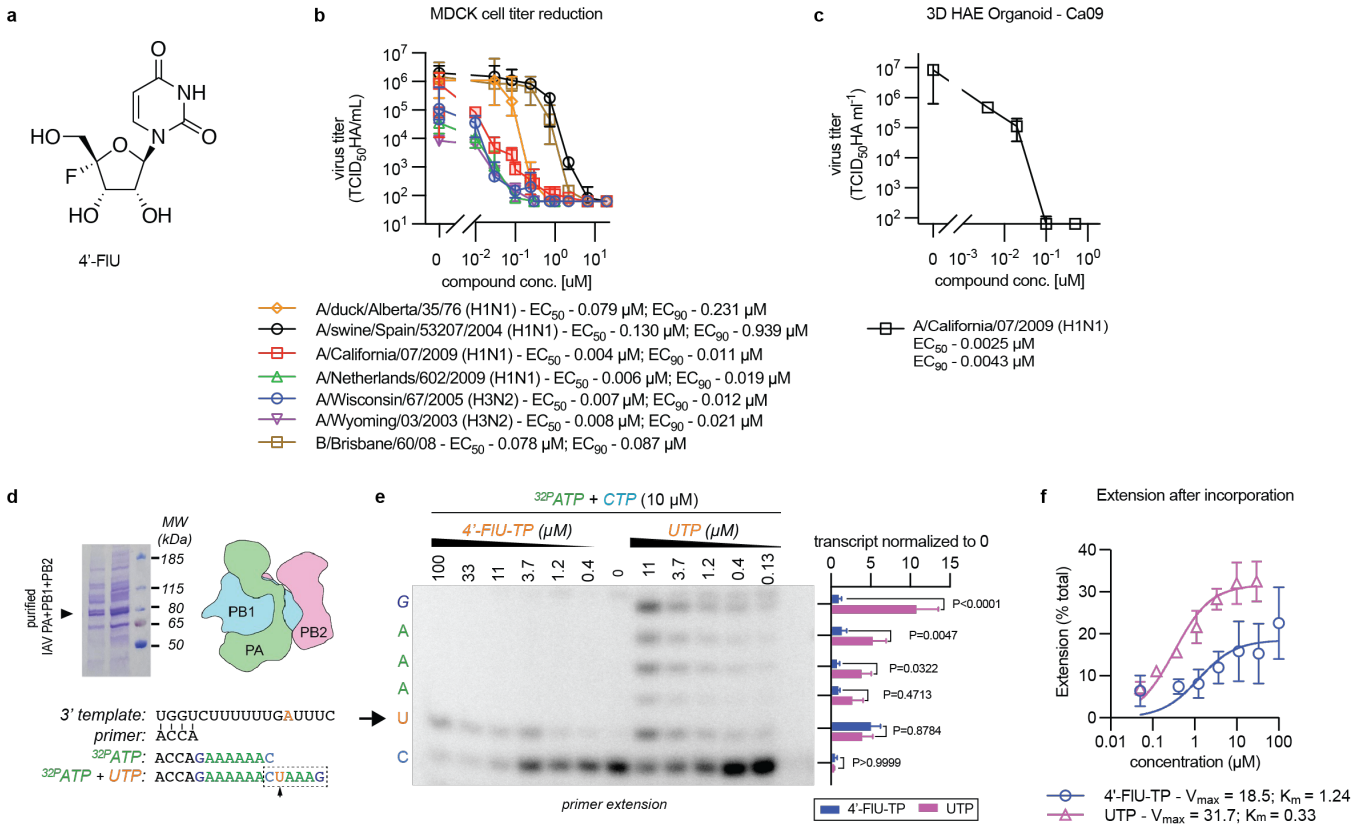
a
4'-FIU
b
MDCK cell titer reduction
virus titer (TCID50HA/mL)
compound conc. [uM]
A/duck/Alberta/35/76 (H1N1) - EC50 - 0.079 µM; EC90 - 0.231 µM
A/swine/Spain/53207/2004 (H1N1) - EC50 - 0.130 µM; EC90 - 0.939 µM
A/California/07/2009 (H1N1) - EC50 - 0.004 µM; EC90 - 0.011 µM
A/Netherlands/602/2009 (H1N1) - EC50 - 0.006 µM; EC90 - 0.019 µM
A/Wisconsin/67/2005 (H3N2) - EC50 - 0.007 µM; EC90 - 0.012 µM
A/Wyoming/03/2003 (H3N2) - EC50 - 0.008 µM; EC90 - 0.021 µM
B/Brisbane/60/08 - EC50 - 0.078 µM; EC90 - 0.087 µM
c
3D HAE Organoid - Ca09
virus titer (TCID50HA ml-1)
compound conc. [uM]
A/California/07/2009 (H1N1)
EC50 - 0.0025 µM
EC90 - 0.0043 µM
d
MW (kDa)
purified IAV PA+PB1+PB2
PB1
PB2
PA
3' template: UGGUCUUUUUUGAUUUC
primer: ACCA
32PATP: ACCAGAAAAAAC
32PATP + UTP: ACCAGAAAAAACUAAAG
e
32PATP + CTP (10 µM)
4'-FIU-TP (µM)
UTP (µM)
transcript normalized to 0
P<0.0001
P=0.0047
P=0.0322
P=0.4713
P=0.8784
P>0.9999
primer extension
4'-FIU-TP
UTP
f
Extension after incorporation
Extension (% total)
concentration (µM)
4'-FIU-TP - Vmax = 18.5; Km = 1.24
UTP - Vmax = 31.7; Km = 0.33

Figure 2

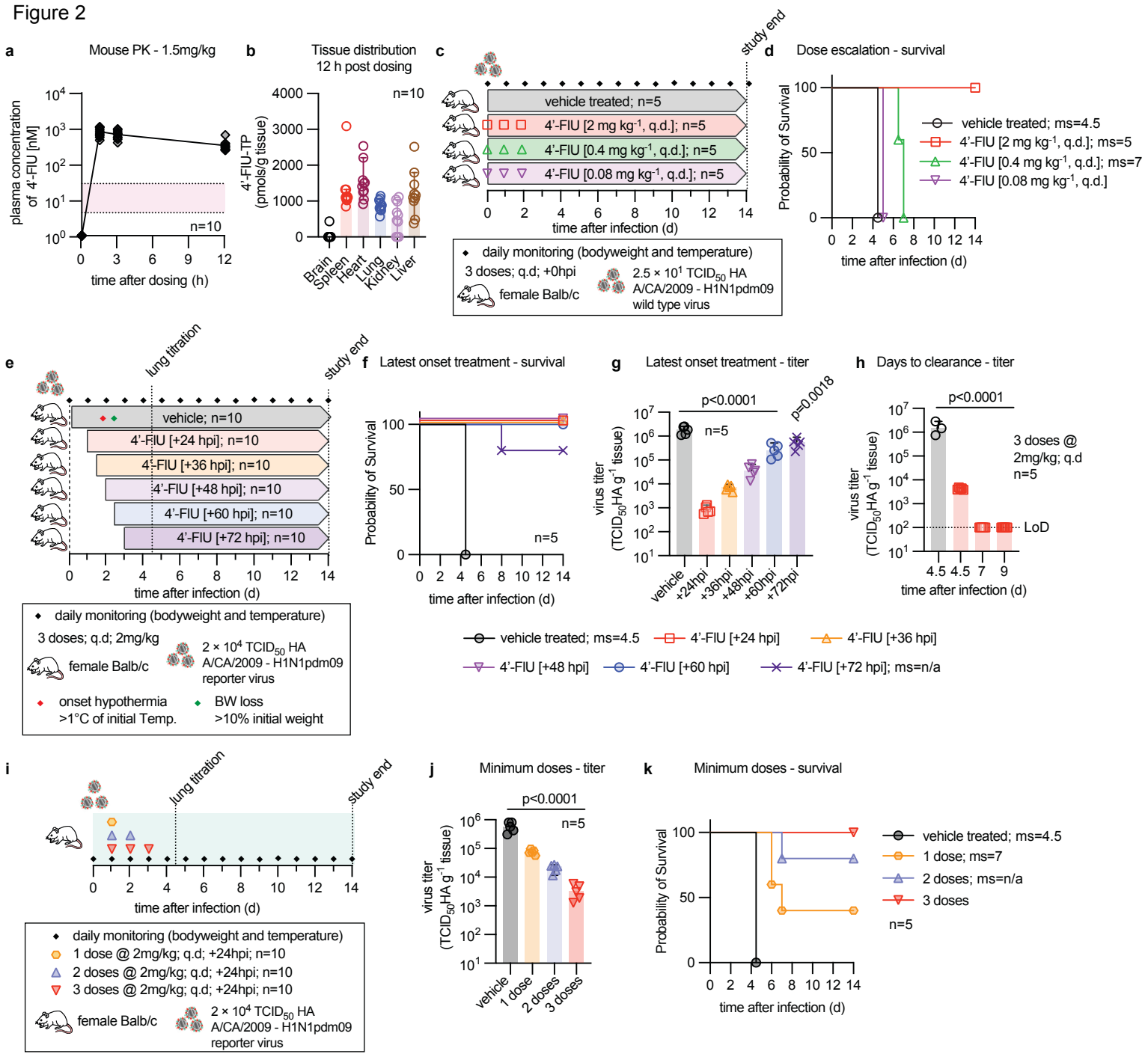
a
Mouse PK - 1.5mg/kg
plasma concentration of 4'-FIU [nM]
n=10
time after dosing (h)
b
Tissue distribution 12 h post dosing
4'-FIU-TP (pmols/g tissue)
n=10
Brain
Spleen
Heart
Lung
Kidney
Liver
c
study end
vehicle treated; n=5
4'-FIU [2 mg kg-1, q.d.]; n=5
4'-FIU [0.4 mg kg-1, q.d.]; n=5
4'-FIU [0.08 mg kg-1, q.d.]; n=5
time after infection (d)
daily monitoring (bodyweight and temperature)
3 doses; q.d; +0hpi
female Balb/c
2.5 × 10^1 TCID50 HA A/CA/2009 - H1N1pdm09 wild type virus
d
Dose escalation - survival
Probability of Survival
vehicle treated; ms=4.5
4'-FIU [2 mg kg-1, q.d.]; ms=5
4'-FIU [0.4 mg kg-1, q.d.]; ms=7
4'-FIU [0.08 mg kg-1, q.d.]
time after infection (d)
e
lung titration
study end
vehicle; n=10
4'-FIU [+24 hpi]; n=10
4'-FIU [+36 hpi]; n=10
4'-FIU [+48 hpi]; n=10
4'-FIU [+60 hpi]; n=10
4'-FIU [+72 hpi]; n=10
time after infection (d)
daily monitoring (bodyweight and temperature)
3 doses; q.d; 2mg/kg
female Balb/c
2 × 10^4 TCID50 HA A/CA/2009 - H1N1pdm09 reporter virus
onset hypothermia >1°C of initial Temp.
BW loss >10% initial weight
f
Latest onset treatment - survival
Probability of Survival
n=5
time after infection (d)
g
Latest onset treatment - titer
p<0.0001
p=0.0018
n=5
virus titer (TCID50HA g-1 tissue)
vehicle
+24hpi
+36hpi
+48hpi
+60hpi
+72hpi
h
Days to clearance - titer
p<0.0001
3 doses @ 2mg/kg; q.d
n=5
LoD
virus titer (TCID50HA g-1 tissue)
time after infection (d)
vehicle treated; ms=4.5
4'-FIU [+24 hpi]
4'-FIU [+36 hpi]
4'-FIU [+48 hpi]
4'-FIU [+60 hpi]
4'-FIU [+72 hpi]; ms=n/a
i
lung titration
study end
time after infection (d)
daily monitoring (bodyweight and temperature)
1 dose @ 2mg/kg; q.d; +24hpi; n=10
2 doses @ 2mg/kg; q.d; +24hpi; n=10
3 doses @ 2mg/kg; q.d; +24hpi; n=10
female Balb/c
2 × 10^4 TCID50 HA A/CA/2009 - H1N1pdm09 reporter virus
j
Minimum doses - titer
p<0.0001
n=5
virus titer (TCID50HA g-1 tissue)
vehicle
1 dose
2 doses
3 doses
k
Minimum doses - survival
Probability of Survival
vehicle treated; ms=4.5
1 dose; ms=7
2 doses; ms=n/a
3 doses
n=5
time after infection (d)

Figure 3

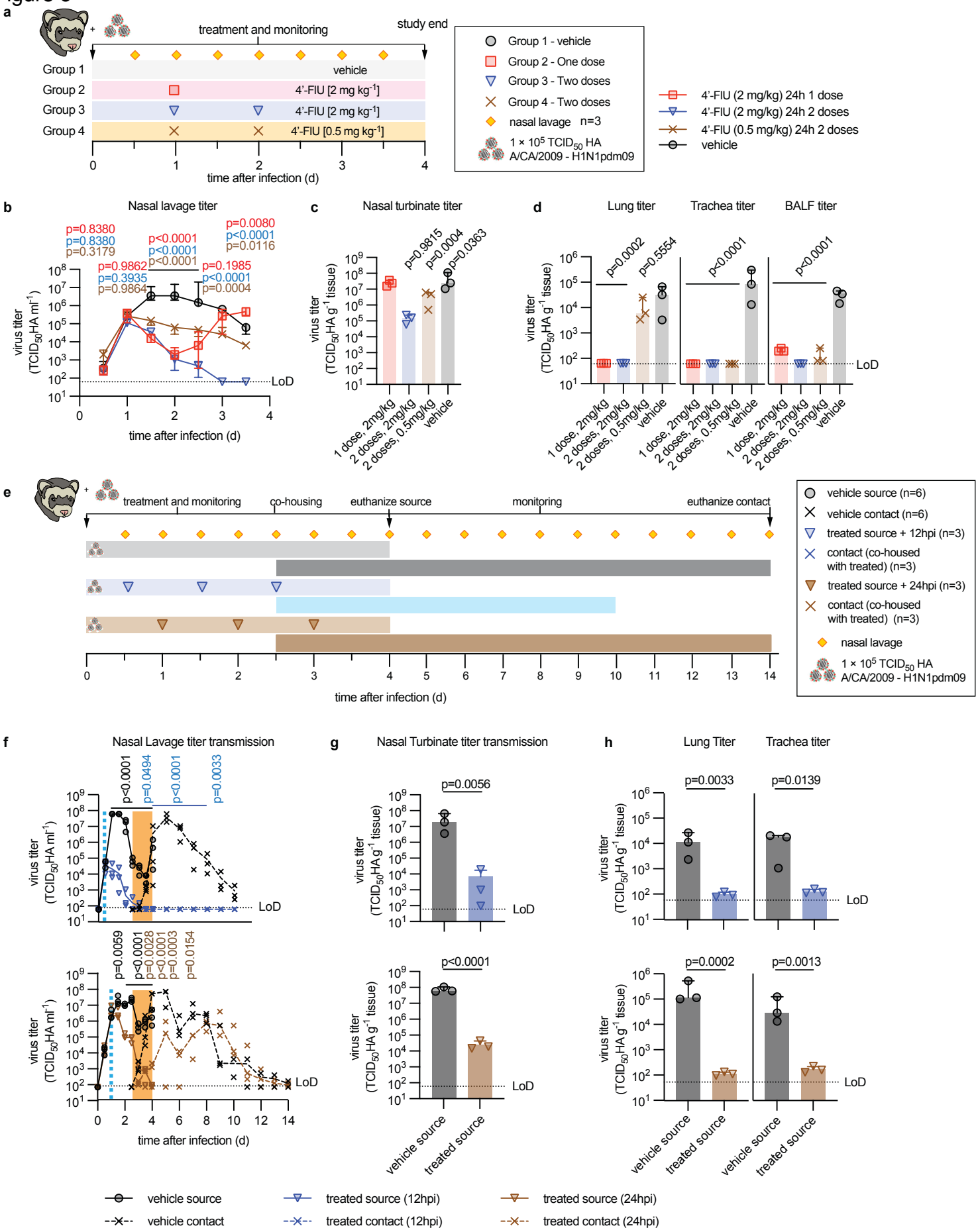
a
treatment and monitoring
study end
Group 1
vehicle
Group 2
4'-FIU [2 mg kg-1]
Group 3
4'-FIU [2 mg kg-1]
Group 4
4'-FIU [0.5 mg kg-1]
time after infection (d)
Group 1 - vehicle
Group 2 - One dose
Group 3 - Two doses
Group 4 - Two doses
nasal lavage n=3
1 × 10^5 TCID50 HA A/CA/2009 - H1N1pdm09
4'-FIU (2 mg/kg) 24h 1 dose
4'-FIU (2 mg/kg) 24h 2 doses
4'-FIU (0.5 mg/kg) 24h 2 doses
vehicle
b
Nasal lavage titer
virus titer (TCID50 HA ml-1)
LoD
time after infection (d)
c
Nasal turbinate titer
virus titer (TCID50 HA g-1 tissue)
p=0.9815
p=0.0004
p=0.0363
1 dose, 2mg/kg
2 doses, 2mg/kg
2 doses, 0.5mg/kg
vehicle
d
Lung titer
Trachea titer
BALF titer
p=0.0002
p=0.5554
p<0.0001
p<0.0001
e
treatment and monitoring
co-housing
euthanize source
monitoring
euthanize contact
vehicle source (n=6)
vehicle contact (n=6)
treated source + 12hpi (n=3)
contact (co-housed with treated) (n=3)
treated source + 24hpi (n=3)
contact (co-housed with treated) (n=3)
nasal lavage
1 × 10^5 TCID50 HA A/CA/2009 - H1N1pdm09
f
Nasal Lavage titer transmission
g
Nasal Turbinate titer transmission
p=0.0056
p<0.0001
h
Lung Titer
Trachea titer
p=0.0033
p=0.0139
p=0.0002
p=0.0013
vehicle source
treated source
vehicle source
vehicle contact
treated source (12hpi)
treated contact (12hpi)
treated source (24hpi)
treated contact (24hpi)

Figure 4

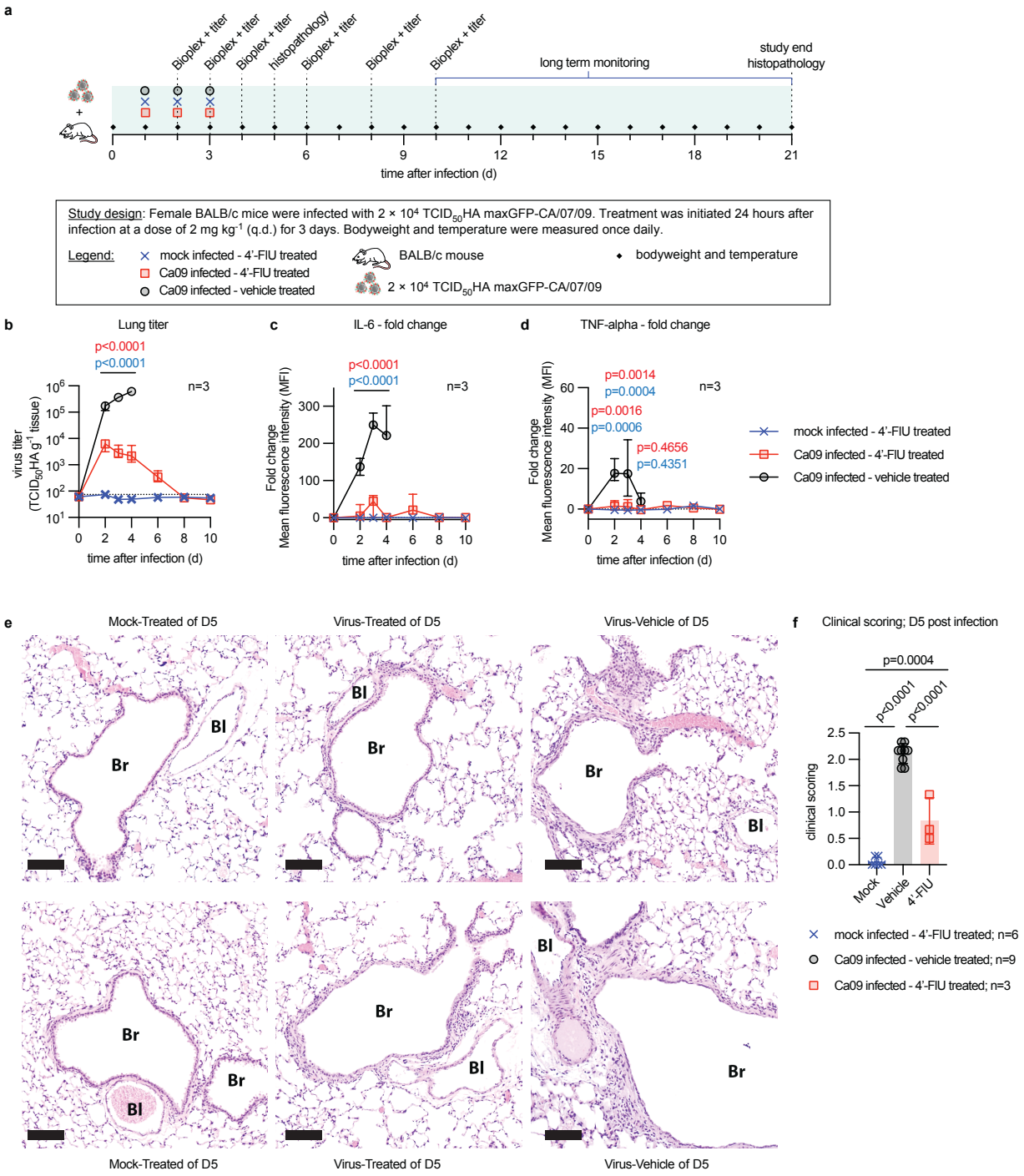
a
Bioplex + titer
Bioplex + titer
Bioplex + titer
histopathology
Bioplex + titer
Bioplex + titer
Bioplex + titer
long term monitoring
study end
histopathology
0
3
6
9
12
15
18
21
time after infection (d)
Study design: Female BALB/c mice were infected with 2 × 10⁴ TCID50HA maxGFP-CA/07/09. Treatment was initiated 24 hours after infection at a dose of 2 mg kg-1 (q.d.) for 3 days. Bodyweight and temperature were measured once daily.
Legend:
mock infected - 4'-FIU treated
Ca09 infected - 4'-FIU treated
Ca09 infected - vehicle treated
BALB/c mouse
2 × 10⁴ TCID50HA maxGFP-CA/07/09
bodyweight and temperature
b
Lung titer
p<0.0001
p<0.0001
n=3
virus titer (TCID50HA g-1 tissue)
time after infection (d)
c
IL-6 - fold change
p<0.0001
p<0.0001
n=3
Fold change Mean fluorescence intensity (MFI)
time after infection (d)
d
TNF-alpha - fold change
p=0.0014
p=0.0004
p=0.0016
p=0.0006
p=0.4656
p=0.4351
n=3
Fold change Mean fluorescence intensity (MFI)
time after infection (d)
mock infected - 4'-FIU treated
Ca09 infected - 4'-FIU treated
Ca09 infected - vehicle treated
e
Mock-Treated of D5
Virus-Treated of D5
Virus-Vehicle of D5
Br
Bl
f
Clinical scoring; D5 post infection
p=0.0004
p<0.0001
p<0.0001
clinical scoring
Mock
Vehicle
4'-FIU
mock infected - 4'-FIU treated; n=6
Ca09 infected - vehicle treated; n=9
Ca09 infected - 4'-FIU treated; n=3

Figure 5

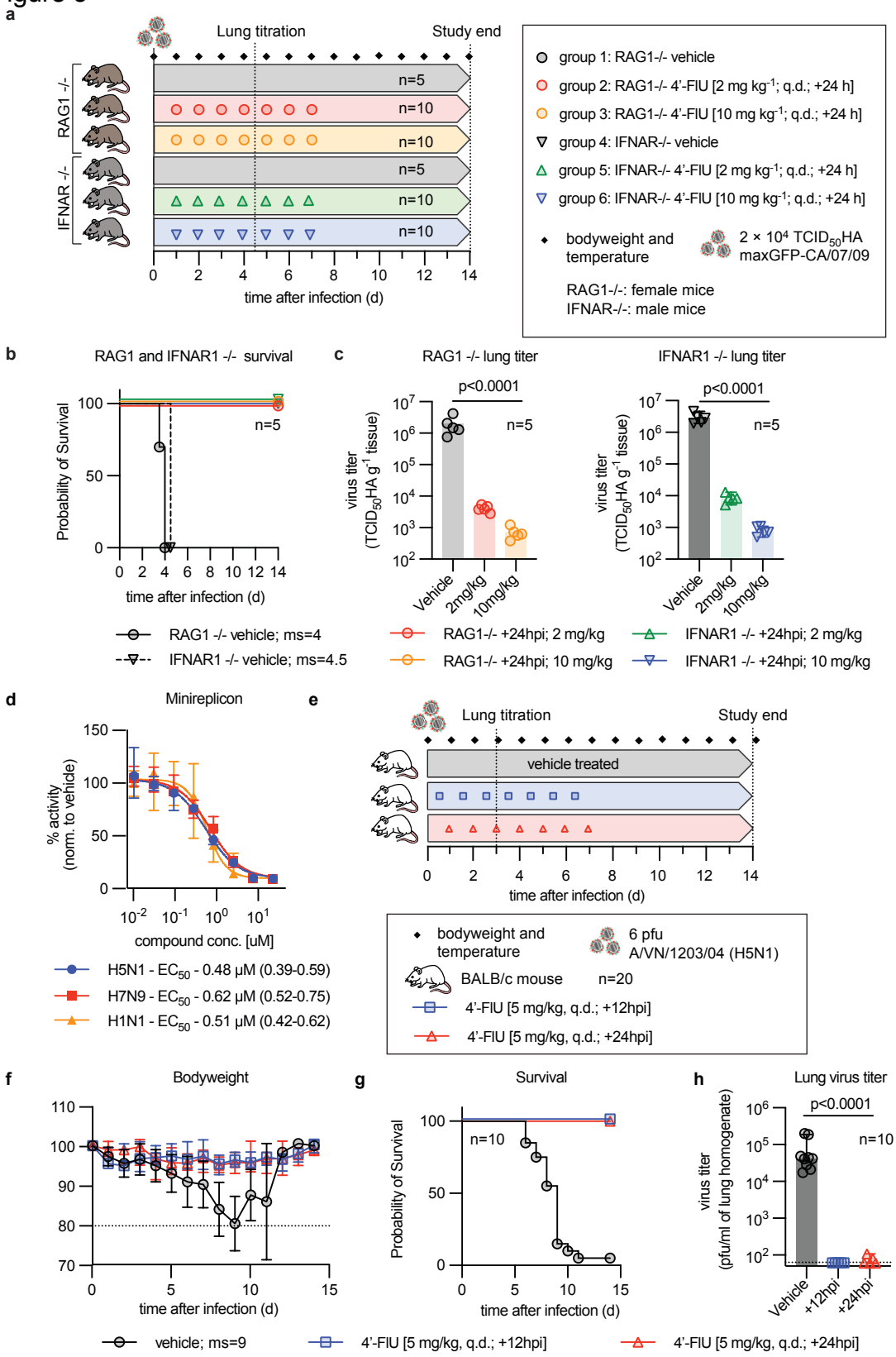
a
Lung titration
Study end
RAG1 -/-
IFNAR -/-
n=5
n=10
n=10
n=5
n=10
n=10
time after infection (d)
group 1: RAG1-/- vehicle
group 2: RAG1-/- 4'-FIU [2 mg kg-1; q.d.; +24 h]
group 3: RAG1-/- 4'-FIU [10 mg kg-1; q.d.; +24 h]
group 4: IFNAR-/- vehicle
group 5: IFNAR-/- 4'-FIU [2 mg kg-1; q.d.; +24 h]
group 6: IFNAR-/- 4'-FIU [10 mg kg-1; q.d.; +24 h]
bodyweight and temperature
2 × 10⁴ TCID50HA maxGFP-CA/07/09
RAG1-/-: female mice
IFNAR-/-: male mice
b
RAG1 and IFNAR1 -/- survival
Probability of Survival
n=5
time after infection (d)
c
RAG1 -/- lung titer
IFNAR1 -/- lung titer
p<0.0001
virus titer (TCID50HA g-1 tissue)
n=5
Vehicle
2mg/kg
10mg/kg
RAG1 -/- vehicle; ms=4
IFNAR1 -/- vehicle; ms=4.5
RAG1-/- +24hpi; 2 mg/kg
RAG1-/- +24hpi; 10 mg/kg
IFNAR1 -/- +24hpi; 2 mg/kg
IFNAR1 -/- +24hpi; 10 mg/kg
d
Minireplicon
% activity (norm. to vehicle)
compound conc. [uM]
H5N1 - EC50 - 0.48 µM (0.39-0.59)
H7N9 - EC50 - 0.62 µM (0.52-0.75)
H1N1 - EC50 - 0.51 µM (0.42-0.62)
e
Lung titration
Study end
vehicle treated
time after infection (d)
bodyweight and temperature
6 pfu A/VN/1203/04 (H5N1)
BALB/c mouse
n=20
4'-FIU [5 mg/kg, q.d.; +12hpi]
4'-FIU [5 mg/kg, q.d.; +24hpi]
f
Bodyweight
time after infection (d)
g
Survival
Probability of Survival
n=10
time after infection (d)
h
Lung virus titer
p<0.0001
virus titer (pfu/ml of lung homogenate)
n=10
Vehicle
+12hpi
+24hpi
vehicle; ms=9
4'-FIU [5 mg/kg, q.d.; +12hpi]
4'-FIU [5 mg/kg, q.d.; +24hpi]

Figure 6

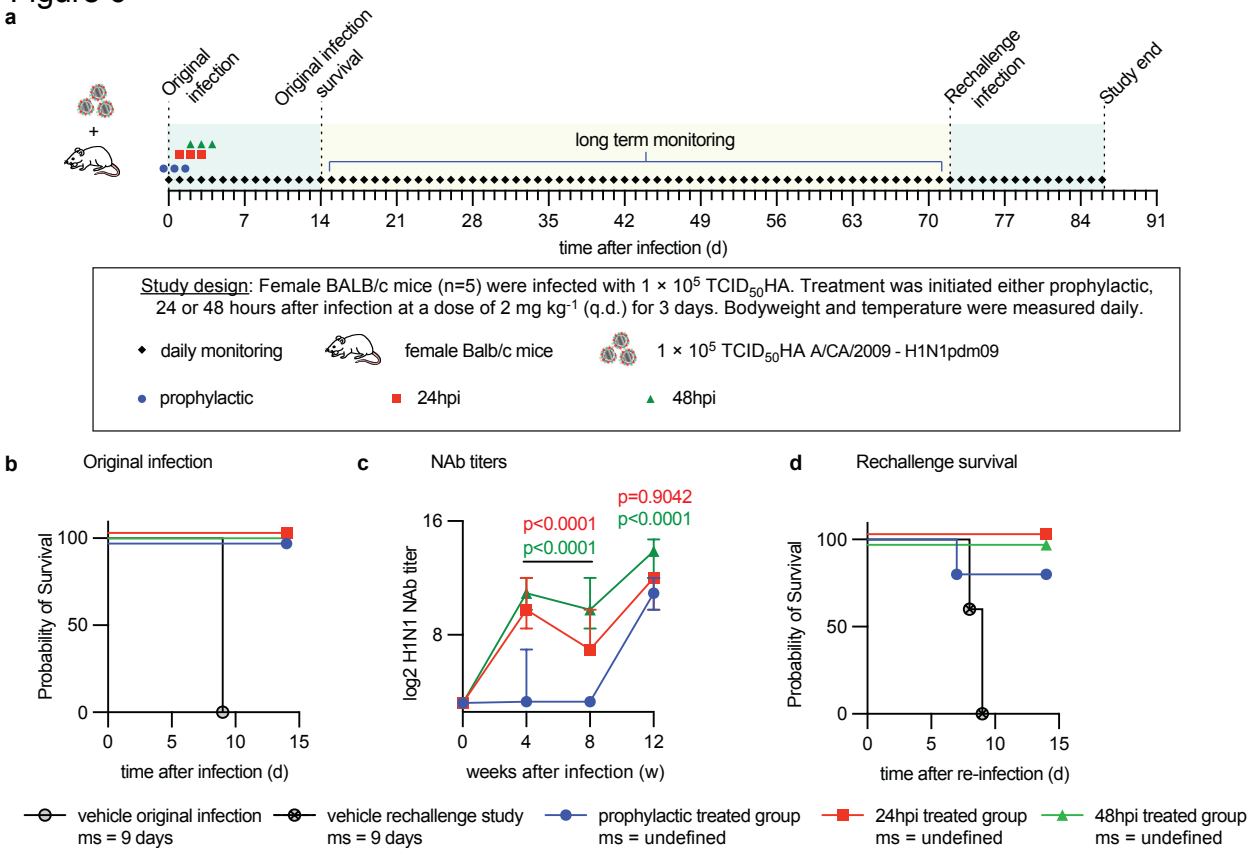
a
Original infection
Original infection survival
Rechallenge infection
Study end
long term monitoring
0
7
14
21
28
35
42
49
56
63
70
77
84
91
time after infection (d)
Study design: Female BALB/c mice (n=5) were infected with 1 × 10^5 TCID50HA. Treatment was initiated either prophylactic, 24 or 48 hours after infection at a dose of 2 mg kg^-1 (q.d.) for 3 days. Bodyweight and temperature were measured daily.
daily monitoring
female Balb/c mice
1 × 10^5 TCID50HA A/CA/2009 - H1N1pdm09
prophylactic
24hpi
48hpi
b
Original infection
Probability of Survival
100
50
0
0
5
10
15
time after infection (d)
c
NAb titers
log2 H1N1 NAb titer
16
8
p<0.0001
p<0.0001
p=0.9042
p<0.0001
0
4
8
12
weeks after infection (w)
d
Rechallenge survival
Probability of Survival
100
50
0
0
5
10
15
time after re-infection (d)
vehicle original infection
ms = 9 days
vehicle rechallenge study
ms = 9 days
prophylactic treated group
ms = undefined
24hpi treated group
ms = undefined
48hpi treated group
ms = undefined